2016

Egg on Hegranes: Geophysical Prospection, Coring, & Test Excavations—Report 2016

John M. Steinberg
University of Massachusetts Boston, john.steinberg@umb.edu

Brian N. Damiata
University of California, Los Angeles

Rita S. Shepard
University of Massachusetts Boston

Kathryn Anne Catlin
Brown University

John W. Schoenfelder
University of Massachusetts Boston

SKAGAFJÖRÐUR CHURCH AND SETTLEMENT SURVEY

Egg on Hegranes: Geophysical Prospection, Coring, & Test Excavations Report 2016

John M. Steinberg
Brian N. Damiata
Rita S. Shepard
Kathryn Catlin
John Schoenfelder
10/31/2016

Photo on front page –Brian Damiata using the GF Instruments' CMD Mini conductivity meter at Egg.

John M. Steinberg, Brian N. Damiata, Rita S. Shepard, Kathryn Catlin &John Schoenfelder

Byggðasafn Skagfirðinga/Fiske Center for Archaeological Research, UMass Boston
BSK 2016-172/ SCASS 2016-6

2016

ACKNOWLEDGEMENTS

We thank the owners of Egg, Embla Dóra Björnsdóttir and Davíð Logi Jónsson for their kind permission and support of the archaeological work. John Steinberg oversaw all work at Egg. Rita Shepard directed the test pit excavations. Brian Damiata directed the geophysical survey. John Schoenfelder oversaw the mapping and kite photography. Kathryn Catlin directed the work at Minna Egg. Davíð Jónsson helped dig and mechanically fill test pits 4 & 5.

General permits for the survey of Hegranes and associated excavations were granted by The Cultural Heritage Agency of Iceland (MÍ201506-0056, MÍ201506-0058, & MÍ201506-0059. The work was supported by the US National Science Foundation (PLR # 1242829, 1345066, 1417772 & 1523025) in a joint project of the Skagafjörður Heritage Museum and UMass Boston. The Icelandic Archaeology Fund also supplied significant support for the project. We are grateful to the Skagafjörður Commune for their ongoing and invaluable support. Any opinions, findings, conclusions, or recommendations expressed in this material are those of the authors and do not necessarily reflect the views of the individuals and institutions who support this work.

SKAGAFJÖRÐUR HERITAGE MUSEUM

The Skagafjörður Heritage Museum is a center for research on local history and cultural heritage in the Skagafjörður region, North Iceland. It is affiliated with the National Museum of Iceland and its main exhibition at the old turf farm of Glaumbær is one of the most visited national heritage tourist attractions. The Archaeological Department of the museum was established in 2003 and engages in contract and research driven archaeology both within and outside the region. The core long-term research programs center on fundamental issues surrounding the settlement and early medieval church history of Skagafjörður and the North-Atlantic region with a focus on developing methodological and theoretical approaches to the geography of early Christian cemeteries. The department is involved in multifaceted interdisciplinary collaboration with Icelandic and international institutions and specialists. Its research portfolio includes bioarchaeology, early metal production, settlement studies, as well as the methodological aspects of archaeological surveying.

FISKE CENTER FOR ARCHAEOLOGICAL RESEARCH

The Andrew Fiske Memorial Center for Archaeological Research at the University of Massachusetts Boston was established in 1999 through the generosity of the late Alice Fiske and her family as a living memorial to her late husband Andrew. As an international leader in interdisciplinary research, the Fiske Center promotes a vision of archaeology as a multi-faceted, theoretically rigorous field that integrates a variety of analytical perspectives into its studies of the cultural and biological dimensions of colonization, urbanization, and industrialization that have occurred over the past one thousand years in the Americas and the Atlantic World. As part of a public university, the Fiske Center maintains a program of local archaeology with a special emphasis on research that meets the needs of cities, towns, and Tribal Nations in New England and the greater Northeast. The Fiske Center also seeks to understand the local as part of a broader Atlantic World.

SKAGAFJÖRÐUR CHURCH AND SETTLEMENT SURVEY

The Skagafjörður Church and Settlement Survey (SCASS) seeks to determine if the settlement pattern of the 9th-century colonization of Iceland effected the development of the religious and economic institutions that dominated the 14th century. The research builds on the combined methods and results of two projects. One has focused on Viking Age settlement patterns. The other has been investigating the changing geography of early Christian cemeteries. Together, the research seeks to understand the connections between the Viking settlement hierarchy and the Christian consolidation.

Contents

List of Figures

List of Tables

1.0 INTRODUCTION

The farm of Egg is in the southernmost part of Hegranes and is bordered on the north by both Keldudalur, and Keta, on the east is Rein (now a part of Egg), Eyhildarholt on the south (which, until recently was not part of Hegranes as Austari-Héraðsvötn has shifted east of Eyhildarholt) and Vestar Héraðsvötn river on the west (Figure 1).

Egg is first mentioned as a farm where a miracle took place, in the appendix to the *Þorláks Saga Byskups* (Hið íslenska Bókmenntafélag 1858:369). According to the story, a girl at Egg was killed after being caught in the reins of a horse. She was brought back to life when her father called upon Saint Þorlákur Þórhallsson. According to these later documents, the account of this miracle was presented to the Althing in A.D. 1199 by Páll Jónsson, bishop of Iceland at the time. In 1388 Egg, along with Rein, is listed in the Hólar land inventory as belonging to that bishopric (Pálsson 2010:123). When Egg was assessed in 1709 as part of the *Járðabók* survey (Magnússon and Vídalín 1930) it was worth 50 hundreds and included the adjacent farms of Rein (abandoned) and Minna Egg (which alone was worth 10 hundreds). According to the *Jarðatal* (Johnsen 1847:277) Mini-Egg and Rein have always been considered part of Egg, which is worth 50 Hundreds for the main farm as well as the sub farms. According to this source, in 1802 Rein was abandoned and a ruin but was part of Egg. Johnsen also claims that Magnússon and Vídalín calculate that Mini Egg was worth 10 hundreds of the 50 hundreds total. According to the *Ny Jardabook* the whole farm was originally worth 50 hundreds but was now, in 1861 revalued to 24.2 hundreds. The main farm of Egg seems to have been continuously occupied since at least 1782 (Pálsson 2010:129). The coring and test excavations described here suggest that Egg was established very early in the settlement sequence.

During the summer of 2016 substantial hand coring, several test pit excavations, kite photography, and geophysical surveys (Figure 2)were conducted at Egg. The work in 2016 was part of the basic SCASS project (described in the front matter), and was implemented to identify and assess the settlement of Egg and determine if there were churchyards.

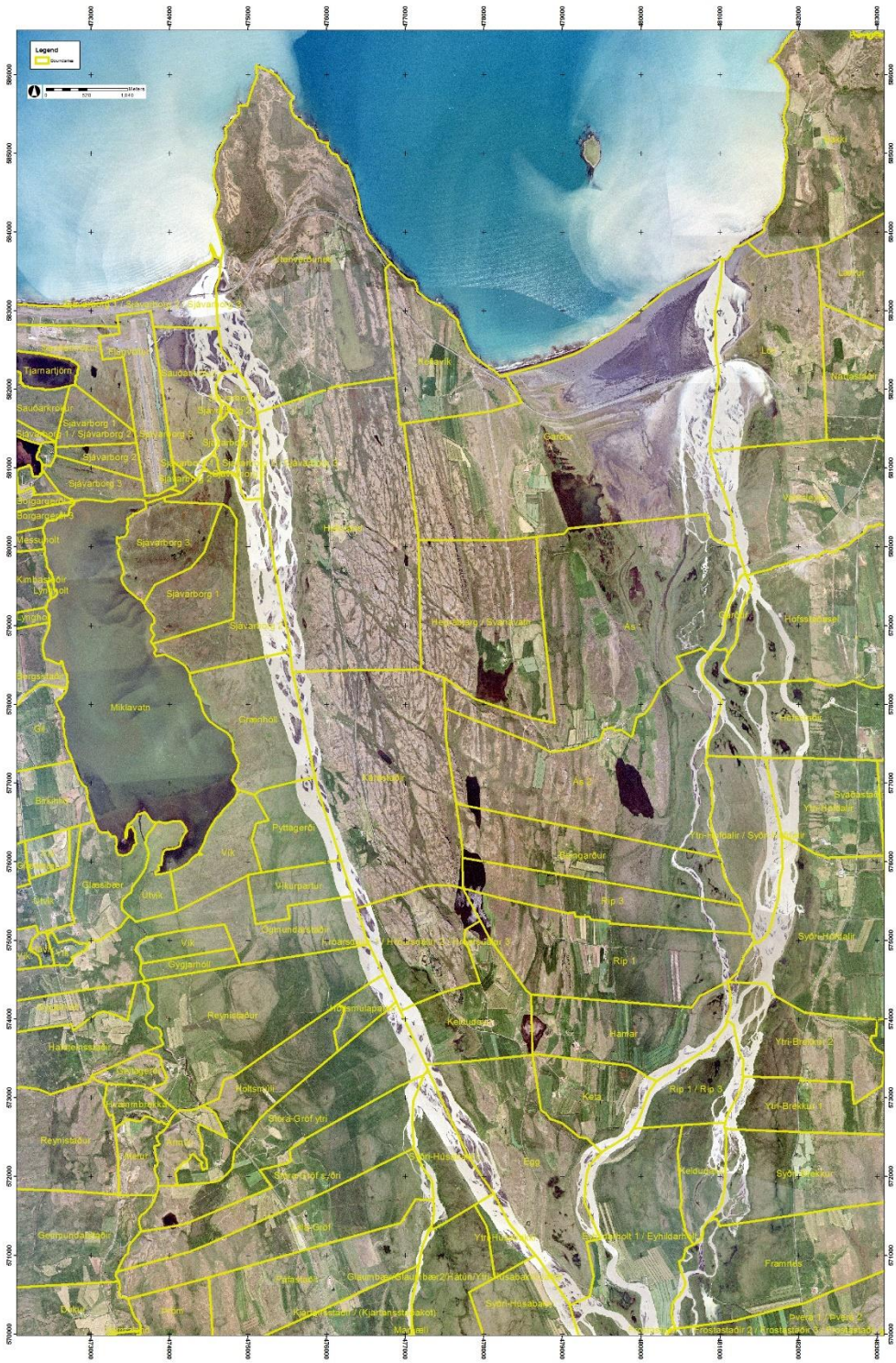

Figure 1. Air photo of Hegranes showing modern farm boundaries in yellow.

1.1 GEOLOGY AND TEPHRA

The geology of the region is characterized by Upper Tertiary basic and intermediate extrusive basalts (Feuillet, et al. 2012) overlain by morainic glacial till. The area was deglaciated by

6100 yr cal.BP and then subject to uplift (Cossart, et al. 2014). The natural stratigraphy of the surface of the region consists of a rapidly formed sediment and soil with intermixed tephra layers, along with gravel layers and lenses of glacial origin. The soil is a brown andosol that derives from aeolian sediments of volcanic origin, but is not the direct product of eruptions (Arnalds 2004, 2008; Arnalds, et al. 1995). The andosol is non-cohesive but has an extremely high water-retention capacity (Arnalds 2008).

The settlement and church survey relies heavily on tephra layers preserved in the soil. Skagafjörður has an early tephra sequence that allows for a fine-grained chronology of the changes in early settlement patterns (Larsen, et al. 2002). While tephra deposition can vary over small distances (Davies, et al. 2010) the basic tephra sequence is found throughout Skagafjörður and allows for a common dating system among farms and farmsteads (Þórarinsson 1977).

- Historic:
  - Hekla A.D. 1766. A black tephra usually found in turf or in the upper 10 cm of the soil sequence.
  - Hekla A.D. 1300: A gray-blue to dark black tephra (Larsen 1984; Larsen, et al. 1999; Larsen, et al. 2002; Larsen, et al. 2001; Sveinbjarnardóttir 1992).
  - Hekla A.D. 1104 (H1). This white or yellowish-white tephra is the most consistent in Skagafjörður (Eiriksson, et al. 2000; Thórarinsson 1967) and is readily identifiable in both natural and cultural stratigraphic sequences.
- Landnám sequence (LNS):
  - Vj~1000 tephra. A blue to bluish-black layer whose source has not been determined but is likely to be either from Grímsvötn or Veiðivötn eruption dated to approximately A.D. 1000 (Boygle 1999; Ólafsson 1985; Sigurgeirsson 1998; Wastegard, et al. 2003).
  - The mid-10th century layer (~950). This blue-green layer is currently an un-sourced and undated layer that is found between the LNL and Vj~1000. There are several potential candidates for this layer, including the large A.D. 934 ±2 eruption of Eldgjá. (Fei and Zhou 2006; Hammer, et al. 1980; Thordarson, et al. 2001) or an A.D. 933 ±6 green tephra layer identified in the Lake Mývatn area from Veiðivötn, termed V-Sv ~950 (Sigurgeirsson, et al. 2013).
  - "Landnám" or "settlement" layer (LNL, LTL, also designated as 871). The layer is so-named for its association with the earliest settlements in Iceland (Dugmore and

Newton 2012)) and is dated to A.D. 871 ±2, (Grönvold, et al. 1995; Zielinski, et al. 1997, [A.D. 877 ±4]). The tephra originates from the Vatnaöldur fissure swarm associated with the Torfajökull and Bárðarbunga volcanos (Dugmore and Newton 2012; Larsen 1984). In general, this layer consists of two distinct tephras–an olive-green tephra overlying a white tephra. However, in Skagafjörður, only the green portion is present (cf. Hallsdóttir 1987).

- Black tephra before the LNL (K800). The earliest tephra in this sequence is a dark black layer probably from the Katla volcano, but is not well dated (Wastegard, et al. 2003). It is usually labled K800 in profiles.

❖ Prehistoric:

- Hekla 3 (H3). A thick (generally 2-3 cm) white or whitish-yellow tephra dating to about 950 B.C. (Dugmore, et al. 1995).
- Hekla 4 (H4). A thick (generally 1-3 cm) white or yellowish-white tephra dating to about 2300 B.C. (Eiriksson, et al. 2000).

1.2 FARMSTEAD STRATIGRAPHY

Chronological phasing of farmstead sizes primarily relies on two tephra layers: the white Hekla A.D. 1104 (H1) and the dark Hekla A.D. 1300. These layers are the most common in coring stratigraphy and often the easiest of the historical tephras to identify. H1 is presented twice as often as Hekla A.D. 1300. Using these tephra layers to date cultural deposits allows for the chronological phasing of farmstead sizes and for farmstead sizes to be compared across contemporary temporal horizons. It also allows for the identification of changes in the size of individual farmsteads. Other tephra layers are used to help identify the overall stratigraphic sequence in the soil cores and to associate specific layers with historical periods. Deposits categorized by these temporal phases based on whether or not they contained "farmstead" material. The resulting chronology allows for the estimation of farmstead size for three primary periods:

- Pre-A.D. 1104
- A.D. 1104-1300
- Post-A.D. 1300

1.3 FARM MOUND DEPOSITS IDENTIFIED IN CORING

Small and infrequent anthropogenic inclusions in soils – such as ash, charcoal, and bone – are common near farmsteads and other activity areas. These are good indicators that an activity area or domestic site may be near but we do not count infrequent inclusions as contributing to the areal extent of the farmstead. Higher concentrations of anthropogenic inclusions, midden deposits, turf, and floors are included. For the purposes of the coring survey, farmstead deposits include:

- Turf deposits: any evidence for a turf structure, including collapsed or levelled turf, are considered evidence of farm buildings. The organic content and percentage of soil in turf deposits is variable. Sometimes tephra layers are present in turf, which can provide a terminus post quem (TPQ) date for the deposit. In general, tephra in turf dates use the tephra identified in the field as a positive farm mound location (yes) for the period(s) after the latest identified tephra. In the absence of in situ tephra, the rest of the deposit is characterized as a potential farm mound (maybe). For example, in a core with turf including what was identified as the H 1300 tephra as the only "farmstead deposit" would be coded as "Yes" for post-1300 but also "Maybe" for the pre-1104 and 1104-1300 phases because of the inherently uncertainty of a field identification of a single dark tephra.
- Low density cultural layers (LDC): defined by anthropogenic inclusions amounting to 10-50% of the soil matrix. These are assumed to result from indistinct and extensive deposition events that suggest regular activity typical of farmsteads or other farm production areas.
- Middens: defined by anthropogenic inclusions amounting to more than 50% of the soil matrix that suggest the regular deposition of household or production area waste. Middens are the result of distinct and intensive deposition events associated with purposeful disposal. In both LDC and Midden layers that are punctuated by tephra layers, for purposes of farm mound dating, the deposits are assumed to be continuous, occurring immediately before and after the date of the tephra deposition. For example, in a midden deposit with only H1 presented, surrounded on either side by midden, both “Pre 1104,” Post 1104,” and “1104-1300” would all be positive (“yes”), while “pre-1000” and “post 1300” would be “maybe.”

- Floor: characterized by dense, compacted, and/or greasy cultural layers indicative of floors, extramural activity areas, or areas of intense deposition of organic materials. These deposits are often thin but are very distinct.

2.0 LAND SURVEYING AND ESTABLISHMENT OF GRIDS

All land-survey data were collected based on the ISN93 coordinate system. Core locations were determined in several manners. Most cores taken away from the modern farm mound used the internal GPS receiver in the iPhone or iPad that was used to collect the coring data. On the farm mound, either a Hiper SR or a Geo XH with Zephier antenna was used to improve the location data collected with the iPad.

Geophysical and excavation grid points were established using a Topcon Hiper SR DGPS using the ISMAR differential station at Stoð ehf. in Sauðárkrókur, which yields about 1 cm accuracy horizontally and 2 cm accuracy vertically. The corner points of the geophysical survey area were flagged using the DGPS. Additional flags were laid out at intervals of 10 x 10 meters using fiberglass measuring tapes that were stretched between the stations established by the DGPS. The eastern and western baselines of the entire grid were flagged at 1-m intervals using alternating colors. Additional lines of alternating flags running east to west were laid out 10 meters apart to help guide the surveying.

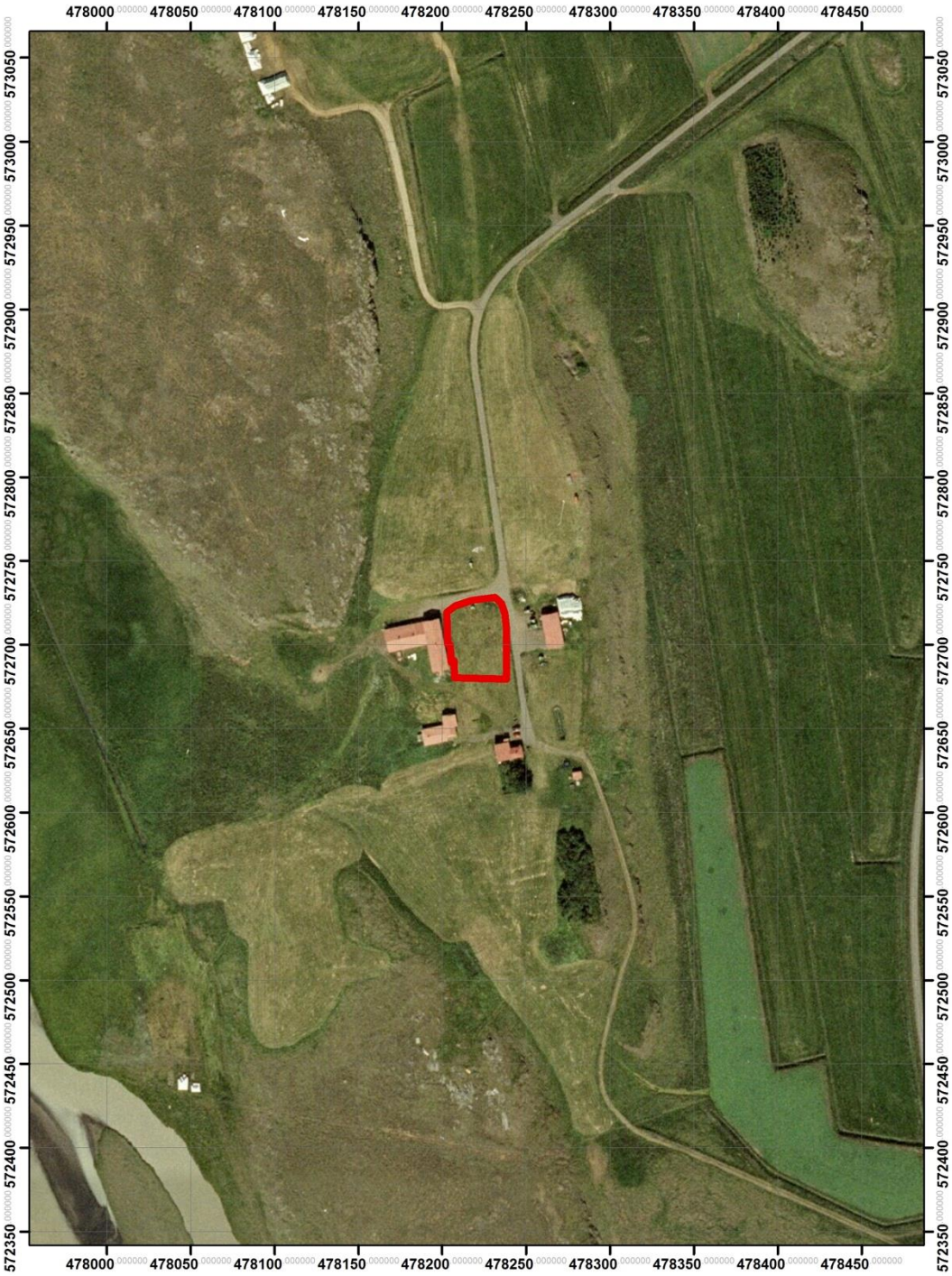

Figure 2. Location of geophysical survey conducted in 2016 at Egg.

3.0 CORING

550 cores were taken at Egg (Figure 3). This does not include work at Rein which is reported on elsewhere. Of those 550 cores, 182 were taken in and around Minna Egg, a small farmstead about 0.5 km south of the main farm mound. The cores at Minna Egg will be reported on as part of the Catlin's Fornbýli project. Coring did not identify any additional sites other than those already recorded (Pálsson 2010) at Egg. The coring did allow us to outline the farm mound extent over broad time periods.

Although much of the land around Egg, has shallow or limited soil, only 17 cores had 10 cm or less of soil accumulation. Sixty-eight of the cores went deeper than 120 cm but 40 of those had H3 or H4 in them. This means that no more than 28 cores did not reach the bottom of the deposits historic sequence, and most of those are in the farm mound itself. Of the 550 cores, 368 had one or more tephra layers in them (Figure 4). Specifically, 284 presented with H3, 158 cores presented H1, and 42 with 1300. Of the 550 cores, 208 presented with some indication of a cultural deposit or cultural activity (Figure 5). Most of the cores with cultural deposits presented at the Farm mound at Egg and at Minna Egg.

There is an area about 80 m south of the main farm mound with some distinct cultural deposits (Figure 6). Only one of these cores (160473) presented a LDC deposit, both above and below the 1104 teprha (Figure 7). The rest of the cores in the area presented turf above the 1104 tephra where present. This suggests primary a post Viking age deposit.

Another area, about 25 m north east and across the road from the main farm mound that has a restricted and compact distribution of cultural deposits. Again there is one core (162175) with LDC above and below an 1104 tephra. Other cores in the area suggest a post 1104 and pre-1300 deposit (Figure 8).

The interpreted coring results from the main farm mound suggest that it has a substantial and extensive pre-1104 component (Figure 9). The primary midden seems to be west of the house and barn (Figure 10), but there are also some midden deposits to the east with shallower deposits immediately north of the greenhouses near Test Pit 2. This would suggest that the central area of the farm mound is under the modern horse paddock, south of the cow barns, and possibly under the cow barns themselves. The blank ("X") cores in and immediately around the horse paddock (Figure 11) experienced refusal, probably due to stones at very shallow depths. This would suggest that either the area has been bulldozed or

that the stones are part of foundations and buildings. The deep cores in a line near Test Trenches 4, 5, & 6 encountered a deposit in the upper 50 cm that, in the cores, appeared to have integrity. However, upon excavation (see section 5.0) the upper deposit was clearly disturbed, probably a fill or bulldozed layer. Thus, the deep cores in this line (Figure 11) are not reflective of the actual deposit. Many of the first cores in this area (e.g., 160177, 160713, 160775, 160779, 160950, 160952, 160953, 160954, & 160961) presented with substantial stones and suggested up cast. These several instances suggested potential grave fill and thus the area was investagated with geophysics (see below).

Farm mound size estimates for Egg are difficult because much of the medieval farm mound must be just south of the modern cow barn, in the horse paddock. Both cores in this area (163320 and 163319) experienced refusal and very shallow depths, but stone alignments in the paddock suggest cultural activities, and the general outline suggests that this is the center of the Egg farm mound. Farm mound extent estimated below the 1104 tephra suggest 20,620 m^2 of material (top right in Figure 12). For the period 1104-1300 AD the farm mound area shrinks by almost 20% to 16,880 m^2. The main farm area is a similar size in post 1300 Egg, at about 16,972 m^2. This may be overstated, as the cores around TP 1 do not suggest significant post 1104 activity, but because they are surrounded by cores that do have positive results for post 1104 activity, that region is included in the farm mound estimates. Because there are three cores with positive results for the presentation of post 1300 cultural deposits in the area just 80 m south the main farm mound, mentioned above, this area (2,431 m^2) should be considered part of the farm mound area during that period (bottom right in Figure 12). Thus, the total farm mound area at post 1300 Egg is 19,403 m^2 (2431+16,972), a 15% increase from the previous period. These numbers suggest that Egg is in the top 4 farms in terms of size, along with Ás, Ríp, and Helluland, in Hegranes.

Table 1. Egg Farm mound areas and centroids

Date	Area (sq m)	Centroid East	Centroid North
Pre-1104	20620	478183	572665
1104-1300	16880	478184	572668
Post-1300	16972	478180	572667
Post-1300	2431	478291	572421

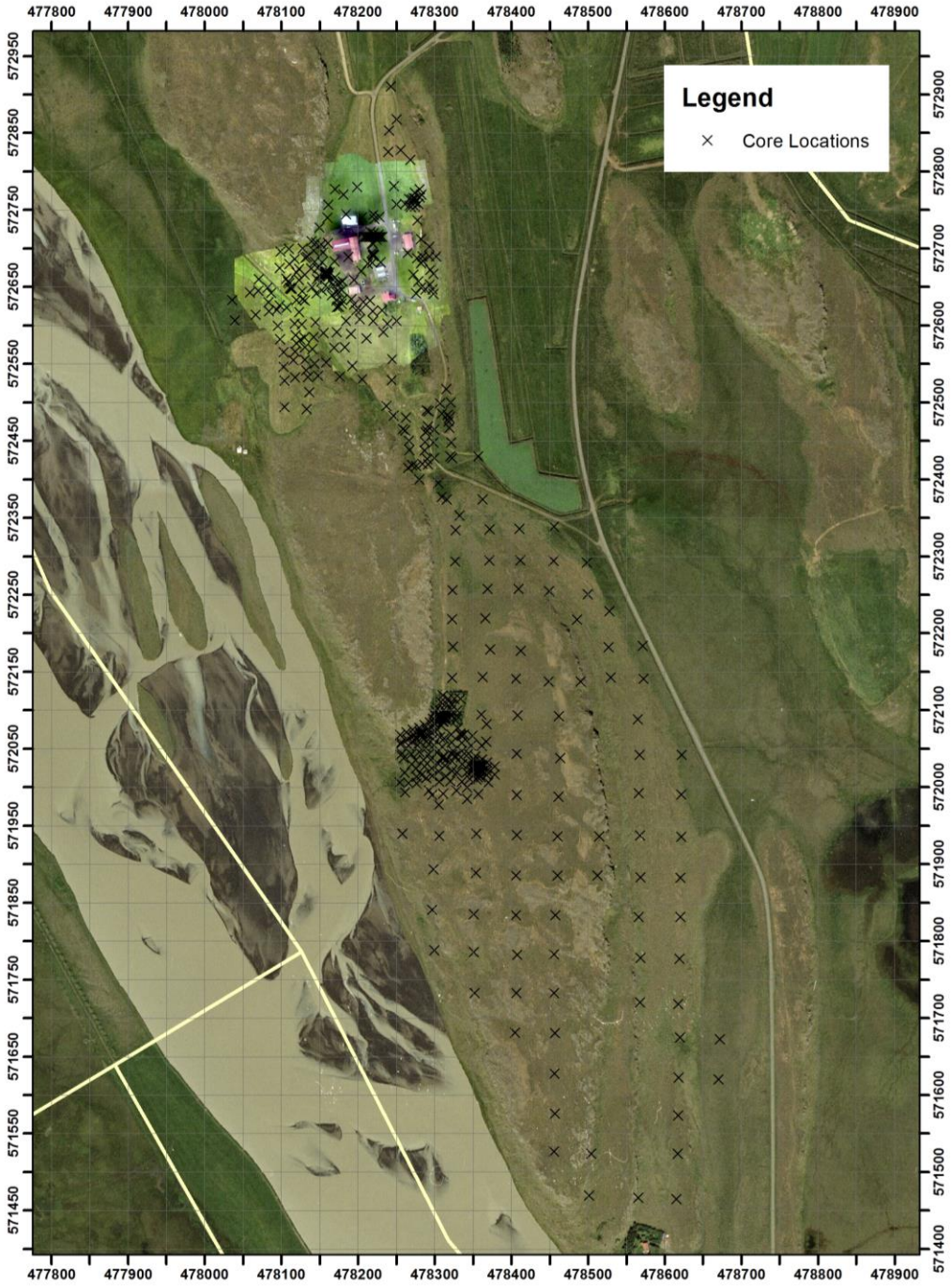

Figure 3. Egg Core Locations

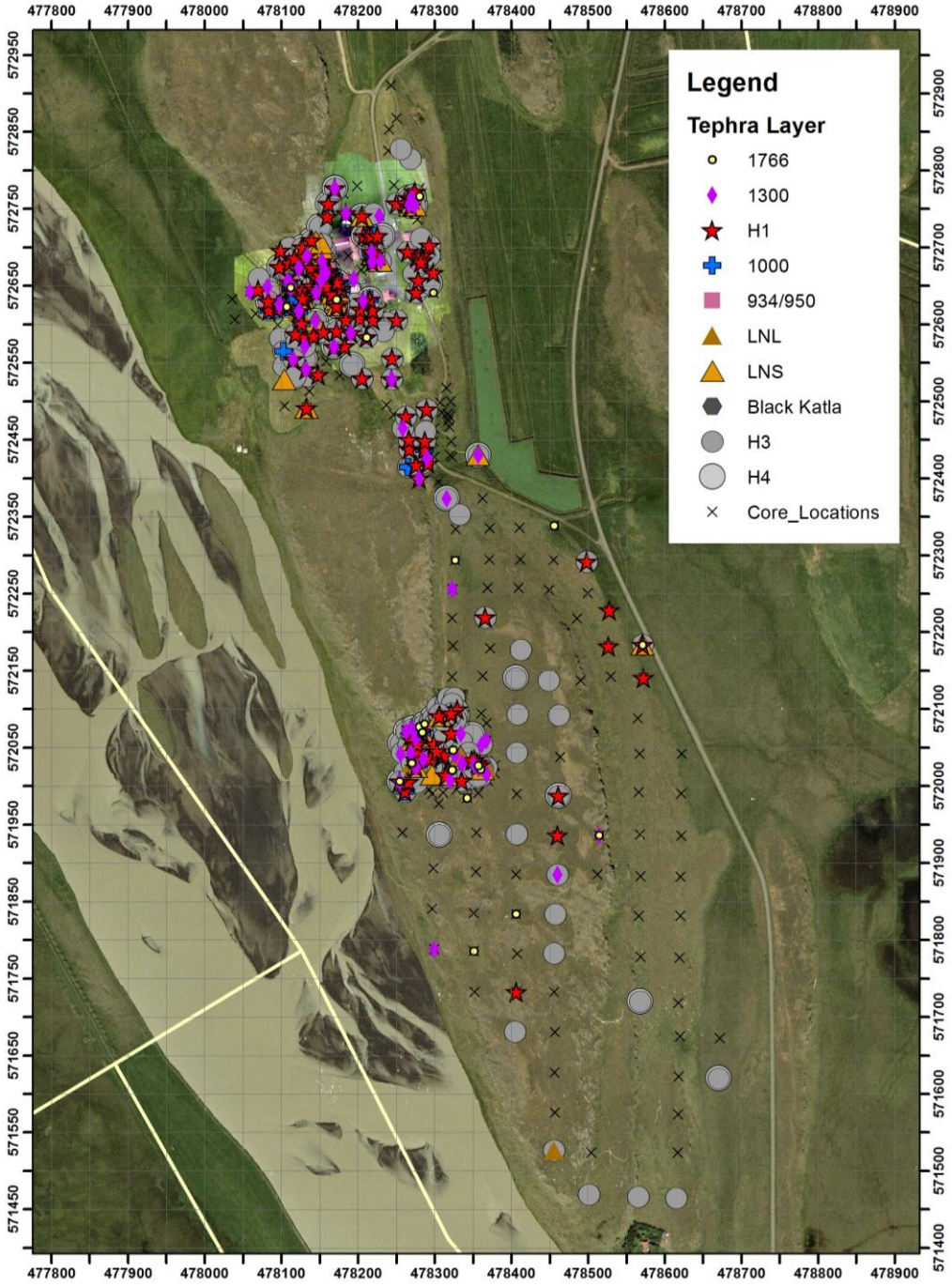

Figure 4.Tephra layers present in cores at Egg

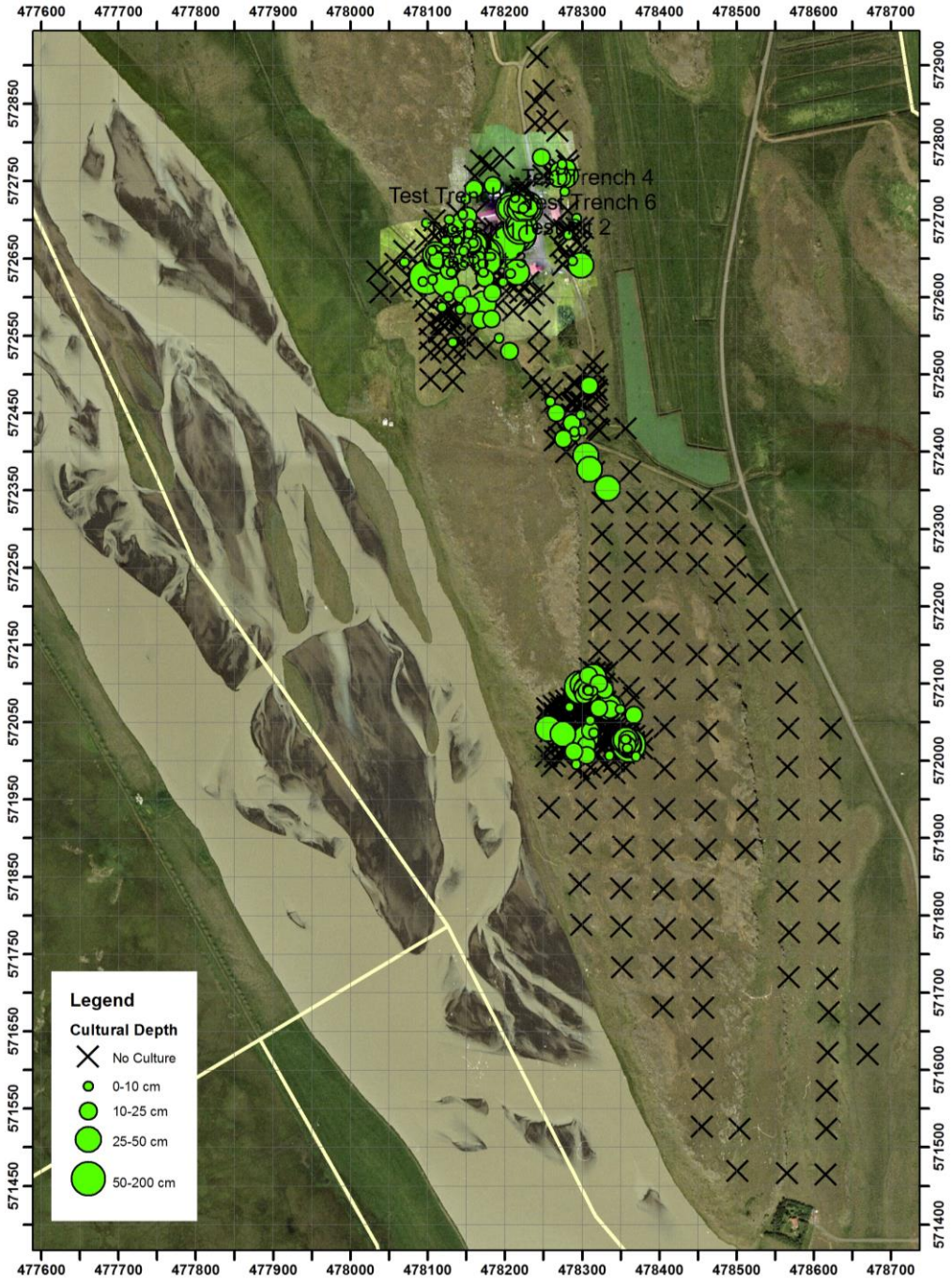

Figure 5. Cultural deposit thickness at Egg.

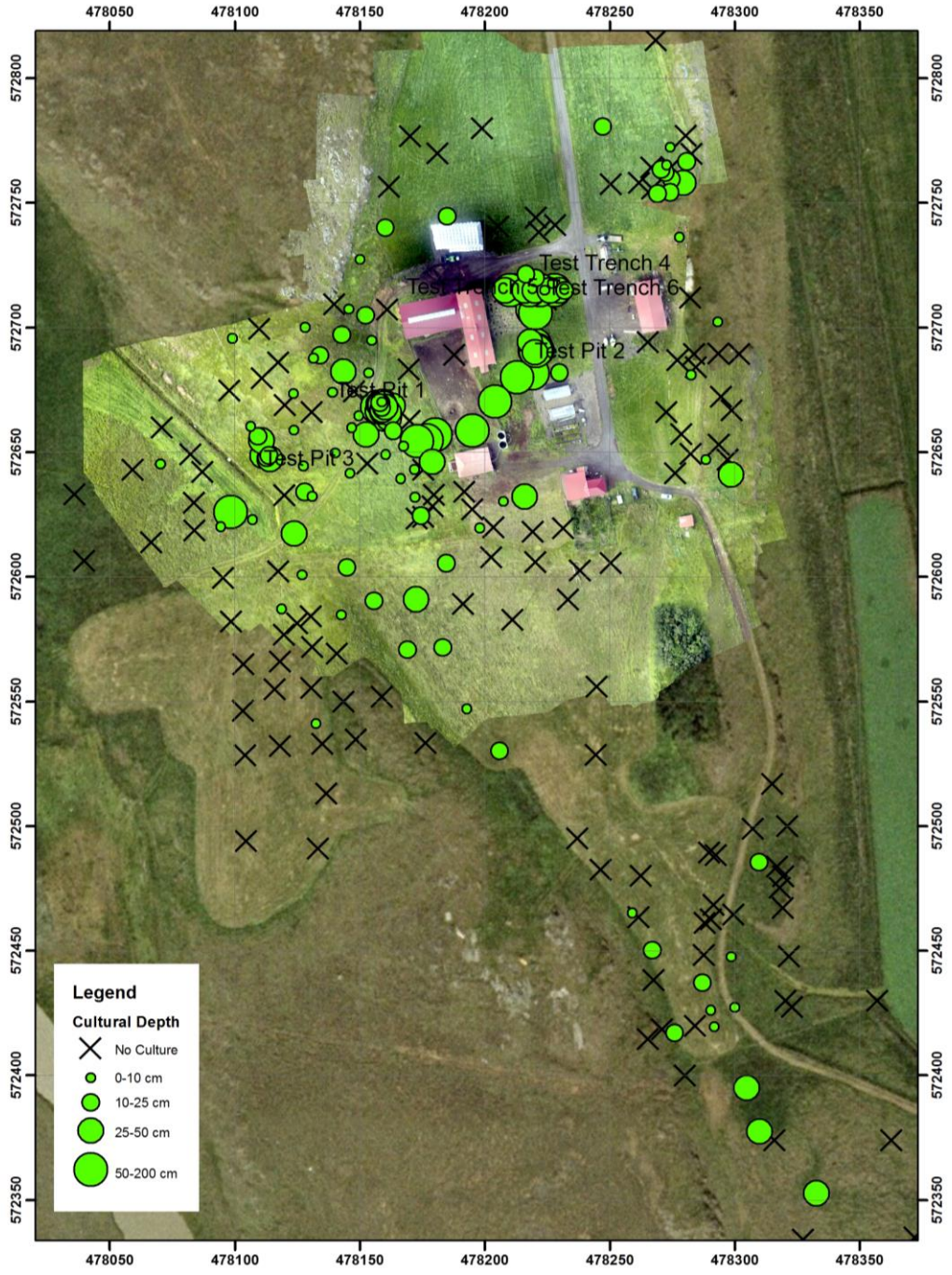

Figure 6.Cultural deposit thickness in the general farm mound area of Egg

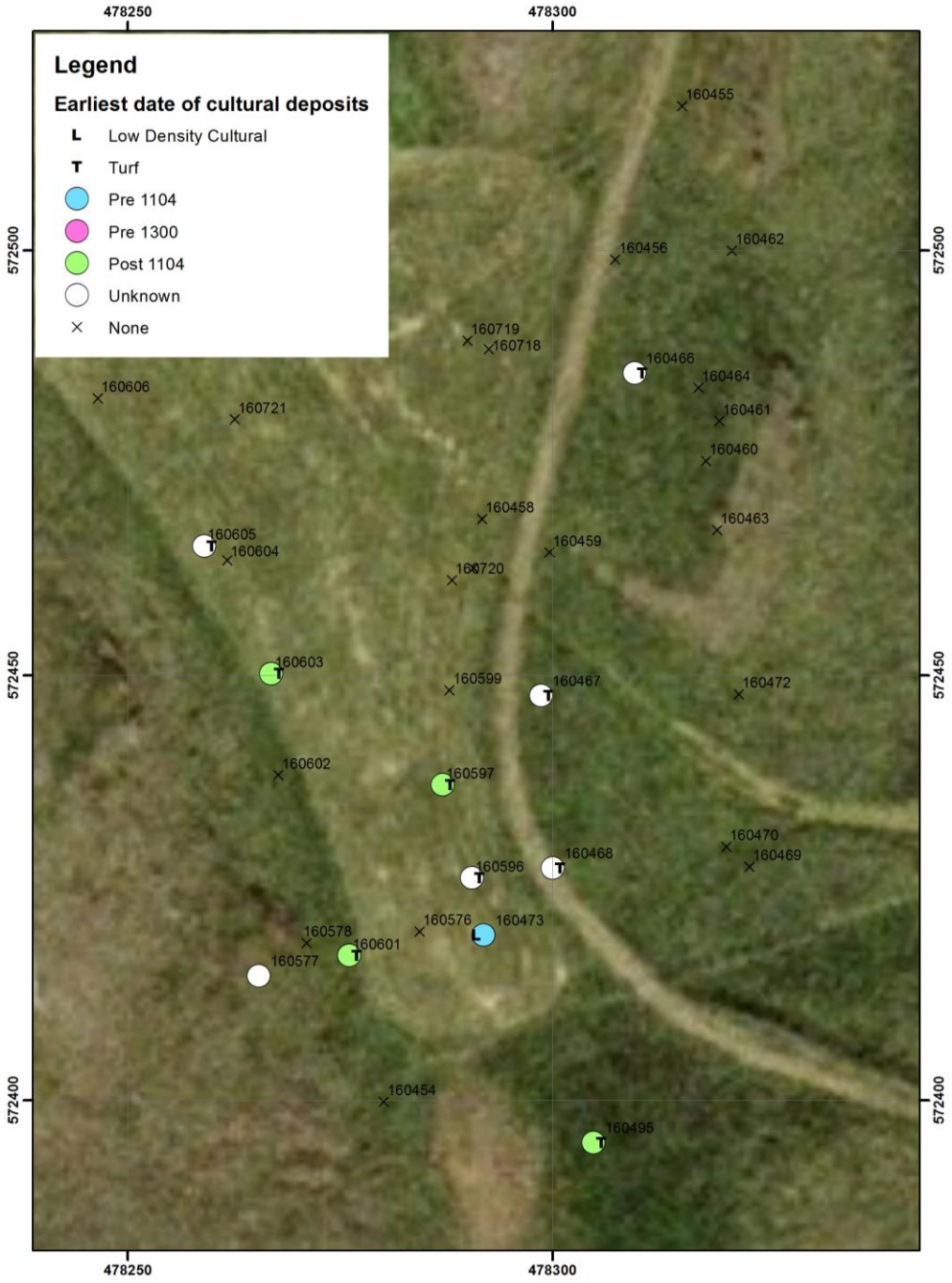

Figure 7. Deposit type and temporal framework of area south of main farm mound.

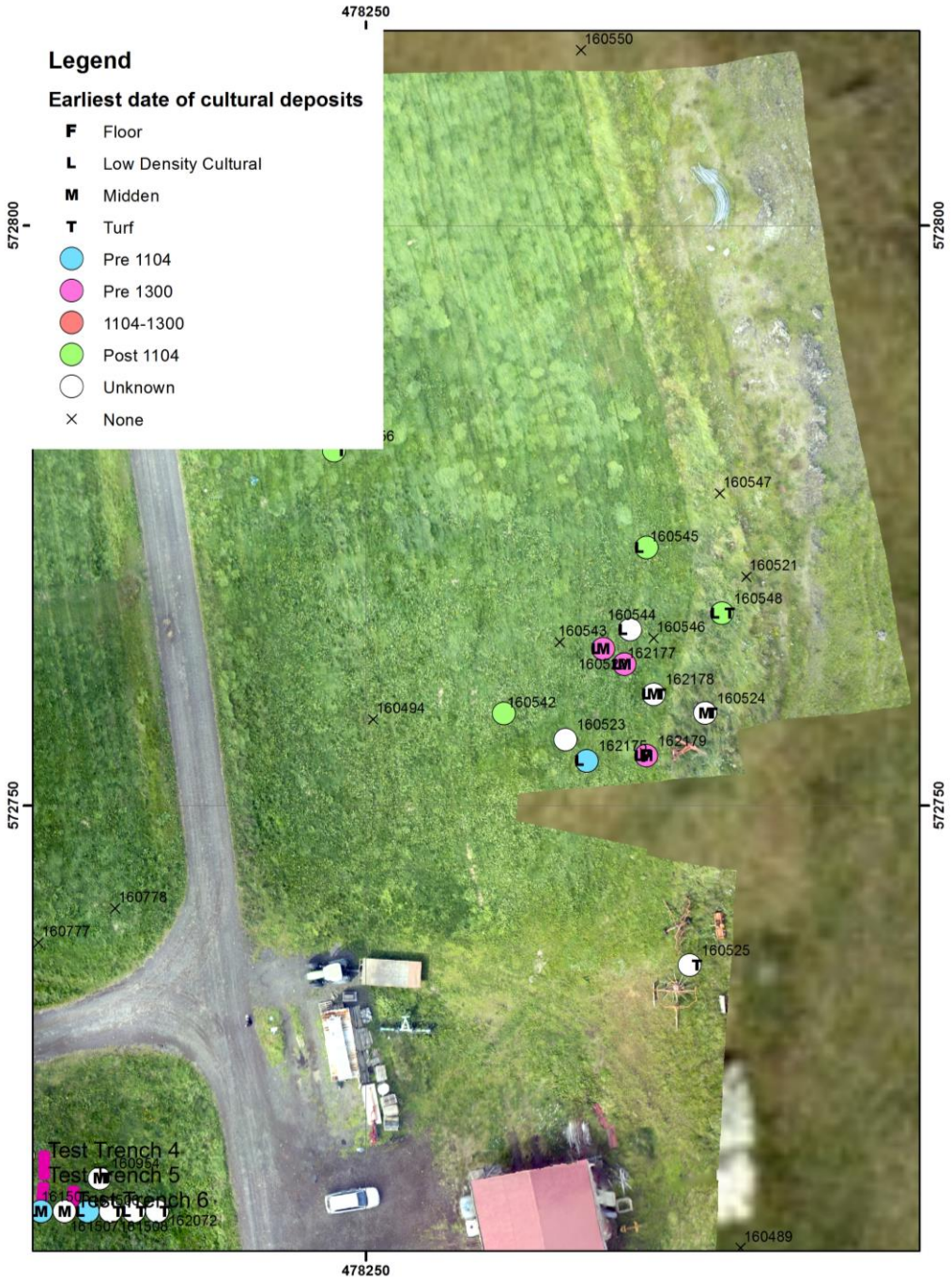

Figure 8. Deposit type and temporal framework of area north of main farm mound.

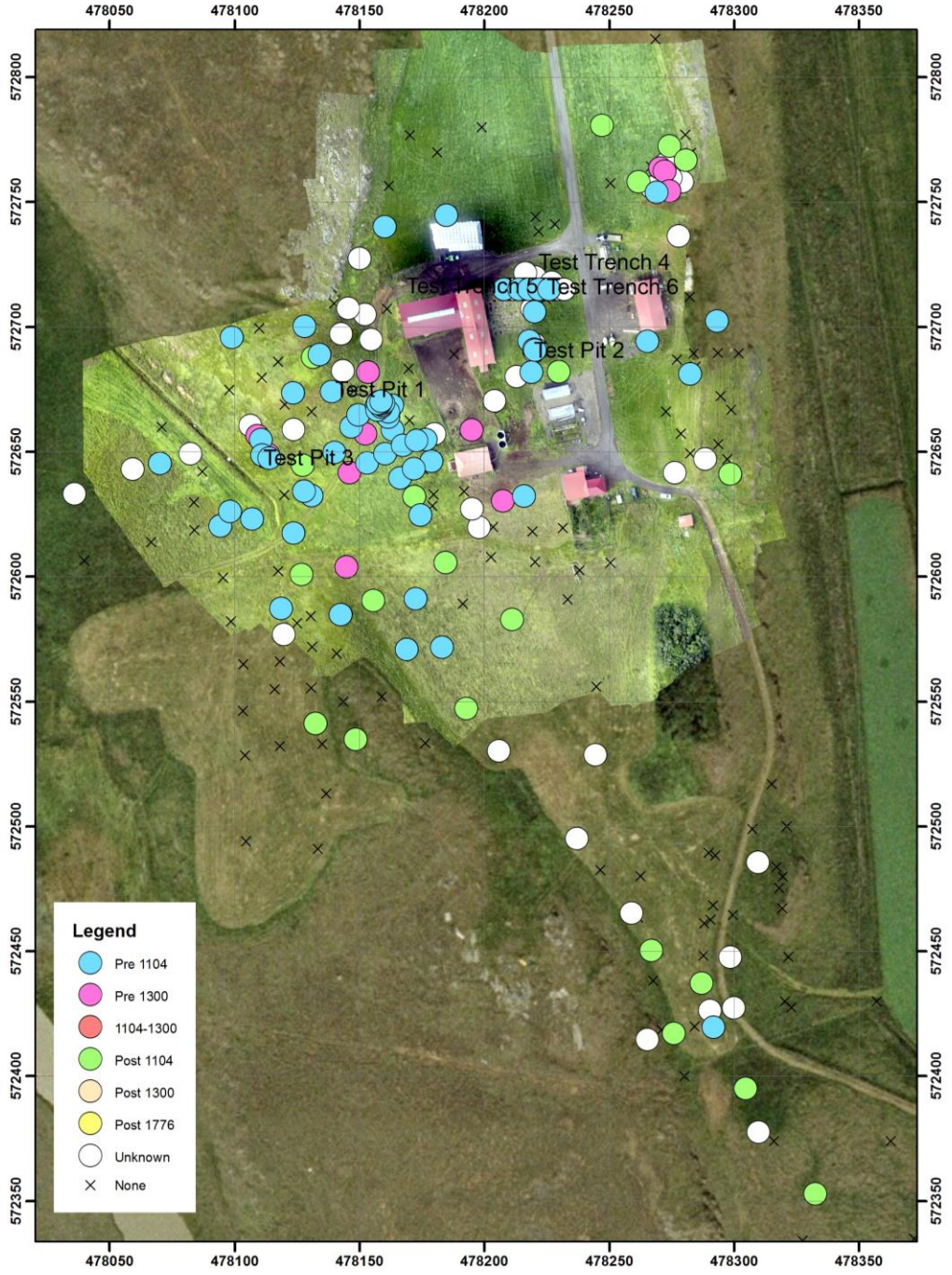

Figure 9. Cultural deposit date in the general farm mound area of Egg

Figure 10.Date and deposit type from cores around farm mound at Egg.

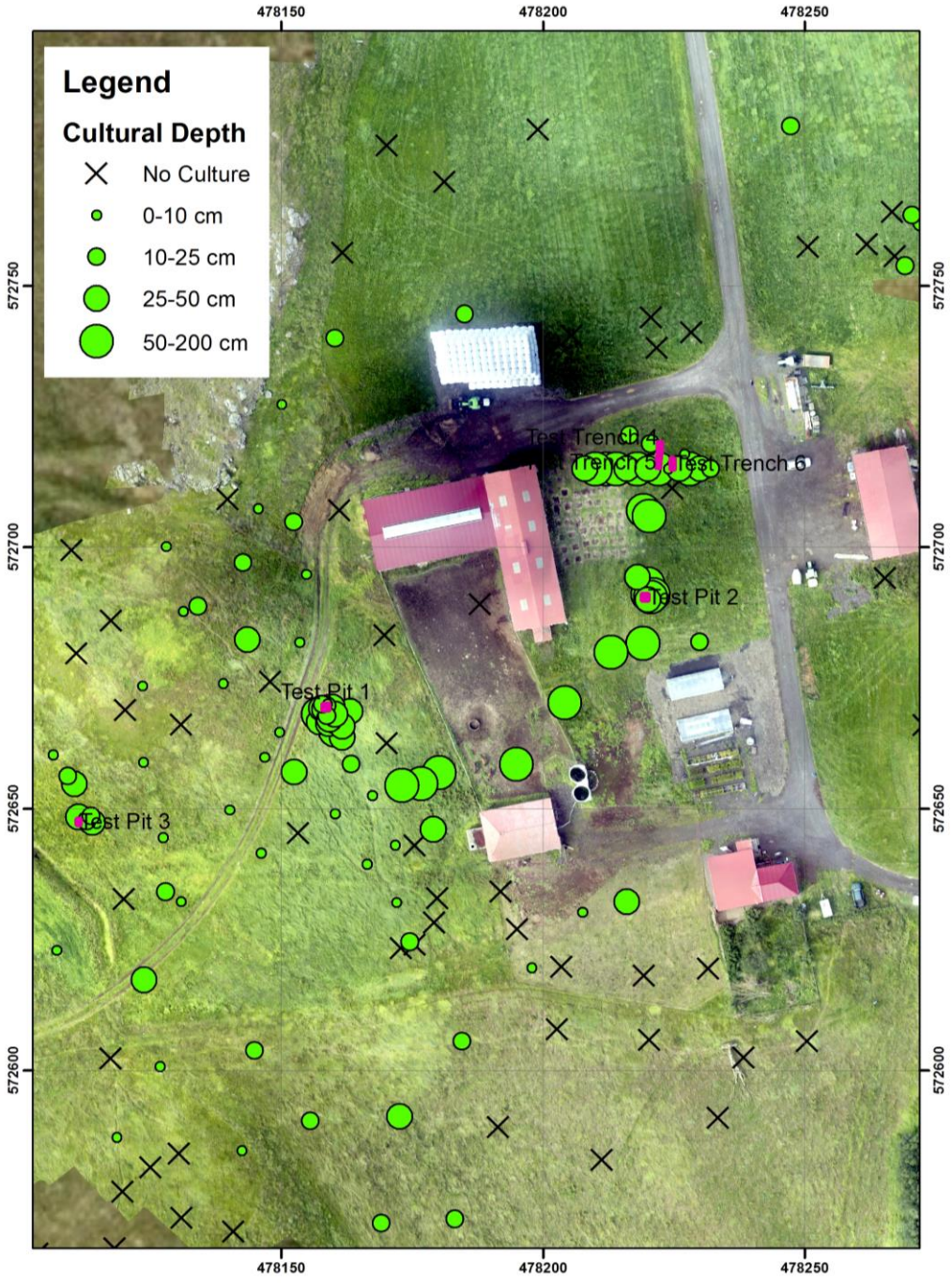

Figure 11. Deposit depth around Egg farm mound.

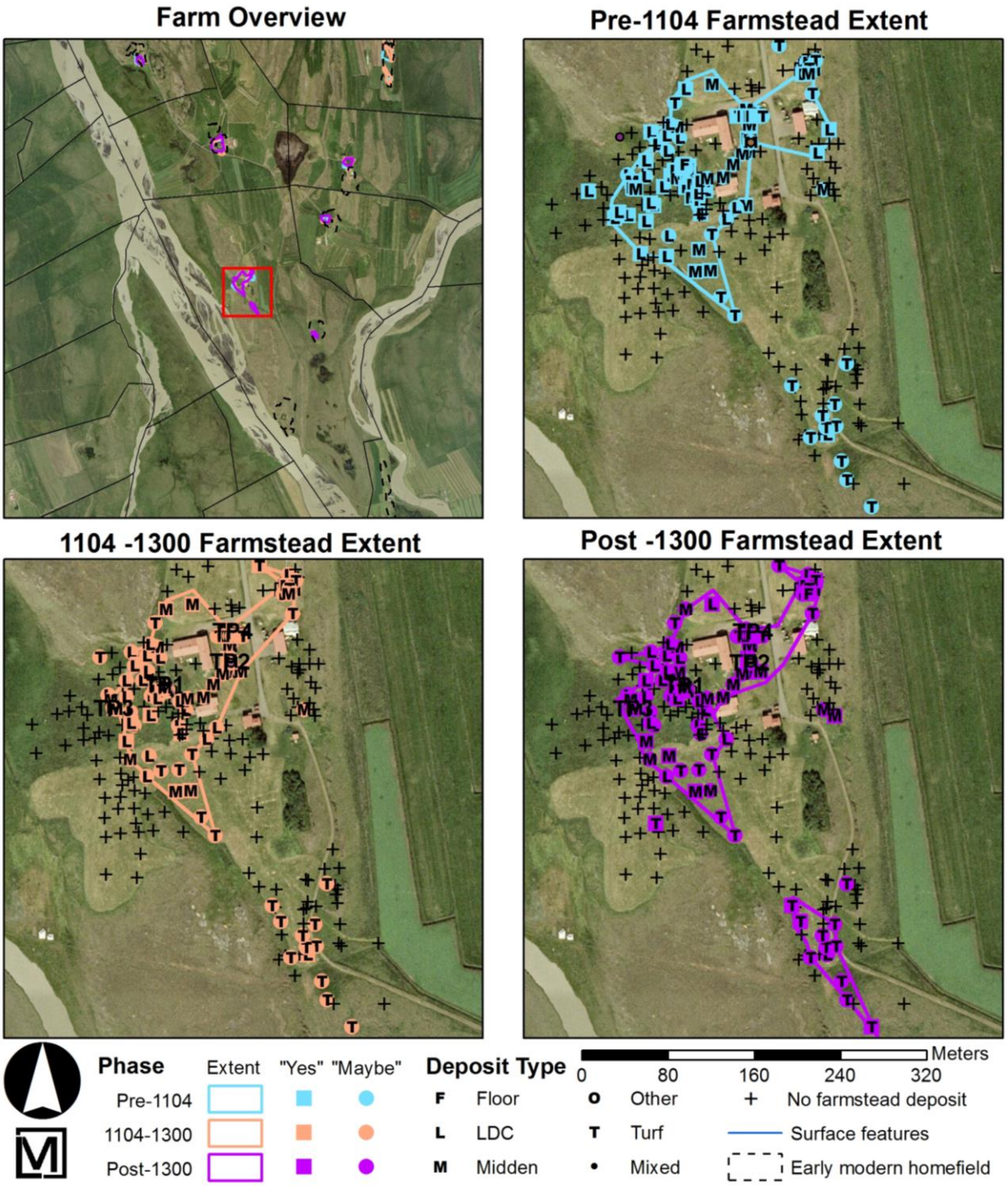

Figure 12. Farm mound extents at Egg. Top left: Egg farm mound in context with other farms in southern Hegranes. Top right: extent of farm mound pre 1104. Bottom left: extent of farm mound 1104-1300. Bottom right: extent of post 13600 farm mound.

4.0 GEOPHYSICAL SURVEY

The use of geophysical methods in support of archaeological investigations is widely established (e.g., Gaffney and Gater 2003; Linford 2006). For the present study, frequency-domain electromagnetics (FDEM),) and ground-penetrating radar (GPR) were applied over portions of the area west of the current cow barn (Figure 1). Summarized below are the geophysical methodologies that were used. Appendices A and B provide general overviews of FDEM and GPR, respectively.

4.1 SITE CONDITIONS AND GEOPHYSICAL TARGETS

There are several potential geophysical targets associated with Viking Age archaeological remains. For this survey, the most important targets are usually found in the central farmstead. The most common include: longhouses, middens, barns, pit houses, outbuildings, and churches. Other features, that are not necessarily buildings, include animal pens and boundary walls, that can, less frequently, be identified using maps of geophysical readings. Geophysical techniques are most effective for predicting the location of buried archaeological structures and deposits without surface sign where the deposits are substantial and are of a single component. Furthermore, the archaeological remains must have physical properties that make them distinct from the surrounding environment. Finally, the geophysical techniques work best where the remains have a will-defined interface with an original surface. Generally, geophysical techniques are contraindicated when the remains are ephemeral, or in disturbed contexts, or part of a complex palimpsest-like deposit.

The two main targets for the geophysical survey are long houses and churchyards. Long houses are distinguishable by their geometry, with two slightly bowed 2 m thick turf walls that are between 4 and 8 m apart. Thus far, we have not identified a central fireplace or hearth with geophysical techniques, but these fire features are a key part of longhouse. Churchyards consist of a small central church that is surrounded by a cemetery, which is enclosed by a circular wall. The churches are often only 3 x 4 m in size and constructed of wood with a stone foundation or post pads. The wall is typically between 15 to 30 m in diameter and composed of compacted turf overlying a stone foundation or gravel base. Graves may be found throughout the enclosed cemetery including under the church. Similarly, other archaeological remains (e.g., booths, walls) are expected to consist of compacted turf blocks overlying a stone foundation. In some cases, the turf will be placed directly on the ground or on a prepared surface without any stones. From a geophysical

perspective, measureable contrasts between stones and soil and between compacted turf and soil are anticipated (i.e., contrast in relative permittivity for GPR and in apparent ground conductivity and in-phase for FDEM).

4.2 FREQUENCY-DOMAIN ELECTROMAGNETIC SURVEYING

In 2016, an FDEM survey was conducted over an irregularly shaped 35 x 45 m grid, just east of the cow barn and west of the main farm road. The GPR survey was conducted on this same grid. The grid was placed to investigate several cores that presented with gravel and potential grave fill (e.g., core 160775) in an area with several known utility lines.

4.2.1 Equipment and Field Procedures

The FDEM surveys were conducted using a GF Instruments' CMD mini-Explorer (Figure 13), which operates at 30 kHz over three separate dipole lengths (i.e., a single transmitter [TX] located at one end of the unit and three separate receivers [RX] located at varying distances along the boom). By increasing dipole length, a greater volume and depth of soil can be sensed. When operated in the vertical dipole mode, the dipole lengths of 0.32, 0.71 and 1.18 m provide depths of interrogation of approximately 0.5, 1.0 and 1.8 m (i.e., ~1.5X the dipole length), respectively, relative to the level of the sensors.

For the surveys, the instrument was operated in the vertical dipole mode with the boom carried at foot level. Data were collected along contiguous transects that were separated by 0.25 m. The sampling rate was set to 10 Hz (i.e., 10 samples per second), which yielded a spacing between measurements of ~0.06 m while walking at a normal pace. Note that surveying was guided by color-coded PVC flags that were placed every 10 meters along transects separated by 1 m. The true location of measurement was determined by fiducial markers that were placed into the data stream by the operator and assuming linear interpolation between markers. Both quadrature phase (bulk ground conductivity) and in-phase (related to bulk ground magnetic susceptibility) components were recorded for each of the three dipole lengths (i.e., six simultaneous readings were recorded for each "measurement"), which yielded about 90,000 readings for each of the two components for each of the three dipole lengths for the surveys in 2016 at Egg.

Figure 13. Using the CMD Mini-Explorer at Egg.

4.2.2 Data Processing

The raw data were initially corrected to properly adjust for the starting and ending locations of each transect. As a check on quality control, the average spacing of measurements for each fiducial segment along a given transect (i.e., every 10 m) was calculated to ensure the spacing between measurements was approximately 0.07 m or less. The data were then processed using Oasis Montaj mapping software to produce grey-shaded and color-contoured maps. The processed data were also archived into a database for future use.

4.2.3 Results

The FDEM survey identified several utilities in the survey area, including the known hot water and electrical lines, as well as 4 other lines, that are probably unused water lines. Most of the lines can be seen in the longest (deepest) dipole readings (e.g., Figure 14 & Figure 15) as well as in the higher measurements (Appendix C). In the in phase readings, near the barn, are a series of blue anomalies that represent the location of hay bales in rows (Figure 14). The FDEM data does show that one of the utility lines terminates in the north central portion of the survey area, (about 478224, 572711) into a 3-4 m anomaly at a location that is noticeable in both the IP and bulk conductivity phases. This anomaly is probably caused by a well and the water line leading out to the south of it. The FDEM results do not suggest any structures of features associated with earlier turf buildings or other structures. That being

said, there does seem to be higher IP readings in the north part of the survey, potentially due to the higher magnetic susceptibility associated with stones and gravel, that may be due to a fill layer identified in the test trenches (see section 5.0)

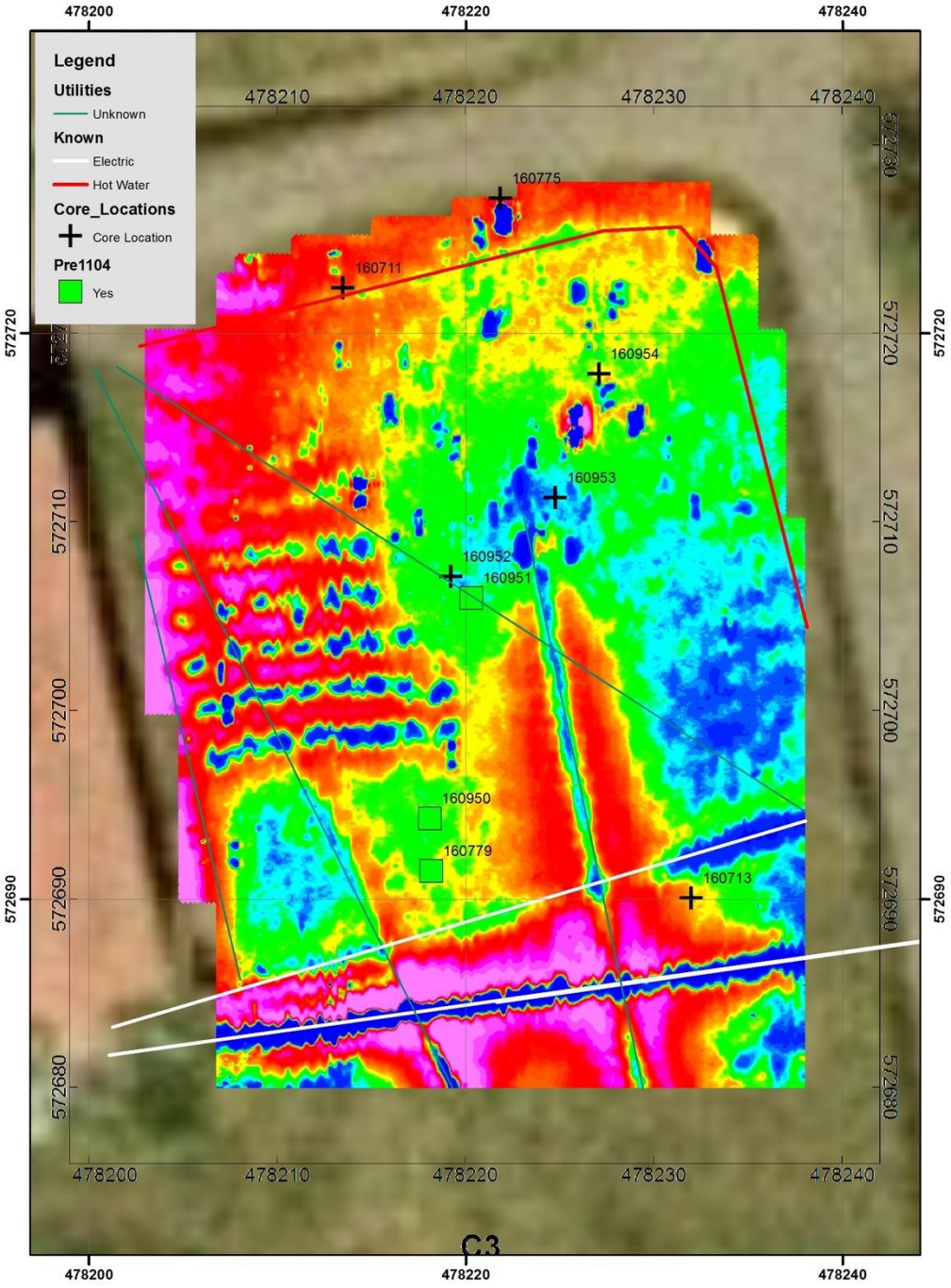

Figure 14. Map of bulk conductivity readings from the CMD-mini using the longest dipole (C3)

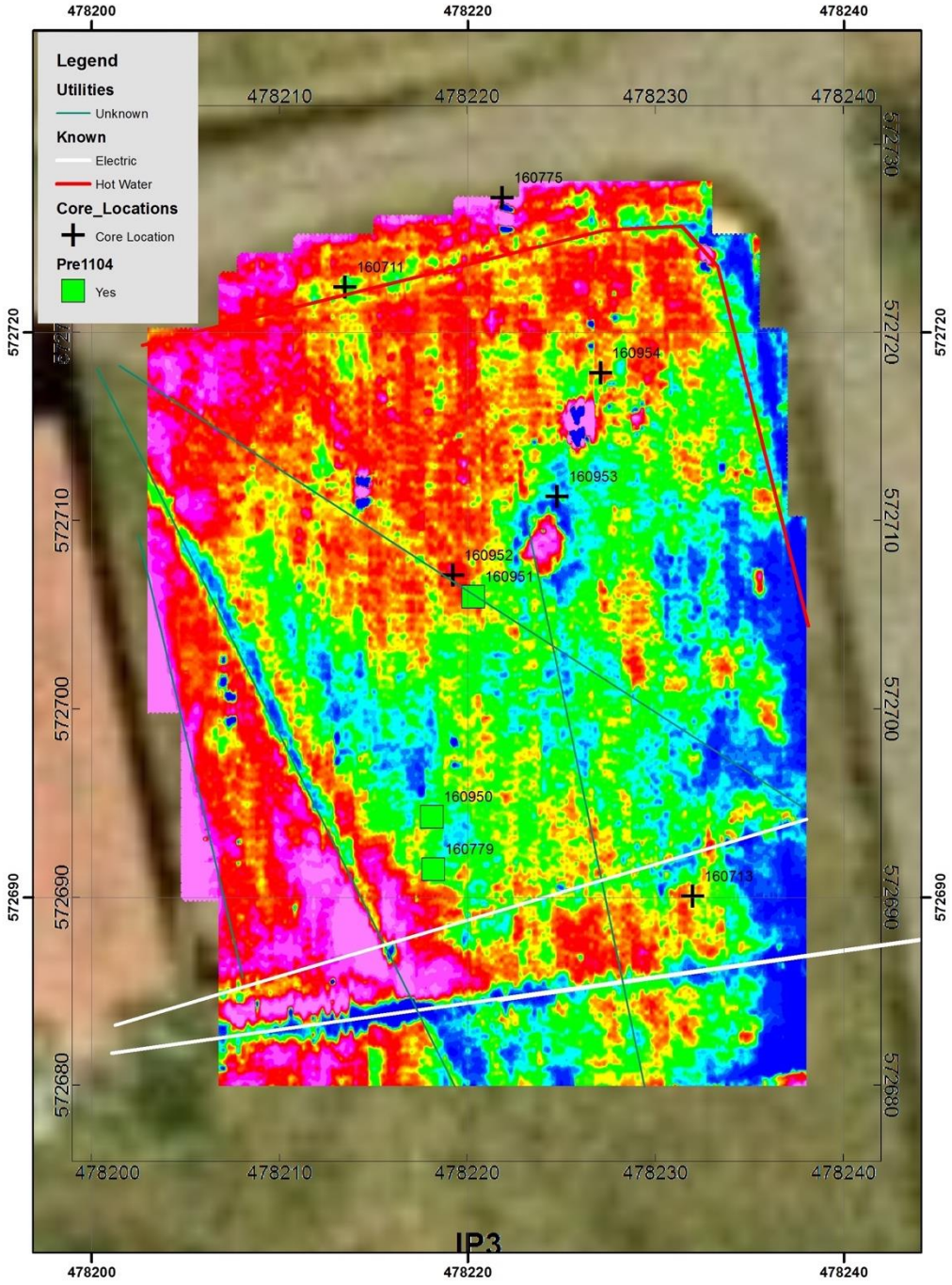

Figure 15. Map of in-phase readings from the CMD-mini using the longest dipole (IP3) with the earliest cores.

4.3 GROUND-PENETRATING RADAR

In 2016, GPR survey was conducted over an irregularly shaped 35 x 45 m grid, just east of the cow barn and west of the main farm road (Figure 2). The FDEM survey was conducted on this same grid. The grid was placed to investigate several cores that presented with gravel and potential grave fill (e.g., core 160775) in an area with several known utility lines.

4.3.1 Equipment and Field Procedures

The GPR survey was performed using a Malå X3M system that was equipped with a 500 MHz antenna (Figure 16). Data were collected at a vertical scan interval of approximately 0.02 m along parallel contiguous transects that were separated by 0.50 m. The data collection was guided by stretching a fiberglass measuring tape between the endpoints of 1-m spaced transects. However, the actual location was determined by a small, lightweight distance-measuring survey wheel with flexible mounts attached to the back of the antenna unit. The survey was conducted in a uni-directional manner (i.e., from south to north). In total, 75 radar profiles (see Appendix D) were collected and about 3,600 linear meters were traversed for the survey.

4.3.2 Data Processing

The data were processed using GPR-Slice software (see www.gpr-survey.com; Goodman, et al. 1995; Goodman, et al. 2008; Goodman, et al. 2007). The raw vertical scan data were gained, resampled and filtered (background removal and boxcar) to produce processed 2-D radargrams (Appendix D). On these radargrams, the presence of strong reflectors is indicated by a black-and-white banding pattern. Note that the raw data were collected in terms of the two-way travel time of reflected energy. To convert to a depth scale, a radar wave velocity of 0.055 m/ns was assumed based on a relative permittivity value of 29.75. The processed radargrams were next combined to produce a pseudo three-dimensional data set. A total of fourty horizontal depth-slice images of approximately 0.05 m with 50% overlap were initially generated to provide detailed spatial information on the location and depth of reflectors (i.e., horizontal plan of strong reflectors at a specific interval of depth that combines data from all radargrams). Overlay depth images were then produced by combining (binning) depth-slice images into 0.25-m-thick intervals, as presented in Figure 17, Figure 18, and Appendix E.

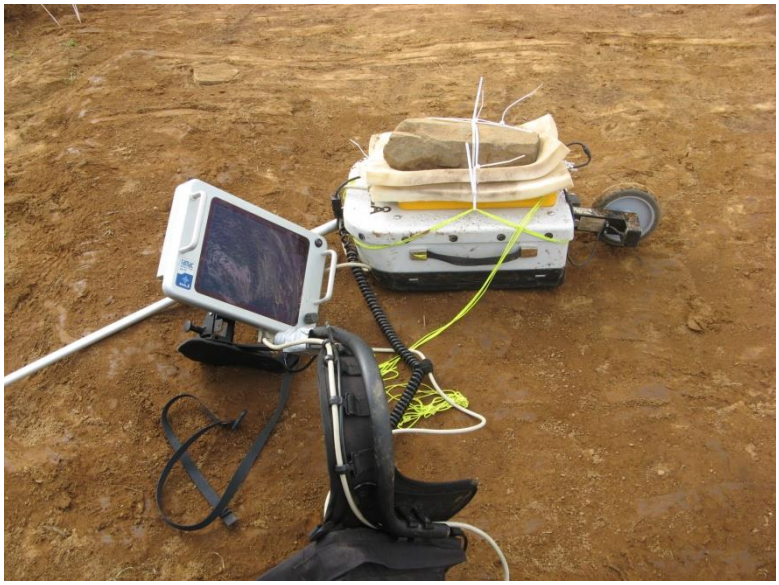

Figure 16. Photograph of the Mala X3 equipped with a 500 MHz antenna.

4.3.3 Results

The GPR results suggested a circular anomaly at about 55 cm bgs (Figure 17) that was consistent in size and shape with a churchyard. The potential well and water line south of it, also identified in the FDEM, was clearly visible as disrupting this circular anomaly, suggesting that the potential well postdated the circular anomaly. Also visible in this slice, as a reflective anomaly (Figure 17), is the utility line running south from the possible well, which could be an unused water line. Several of the other utility lines are also visible, but rather as blue streaks through the yellow and read reflective anomalies. At deeper depths (e.g., Figure 18) a circular anomaly replaces the center hole in the reflective ring. Excavations (described below on page 46) suggest that this ring is a fill deposit and not associated with structural remains. The GPR results do suggest that there may be some intact structural remains south of test pit 2 in between and south of the identified buried electrical lines. These strong reflectors are consistent with stones and may represent some sort of foundation.

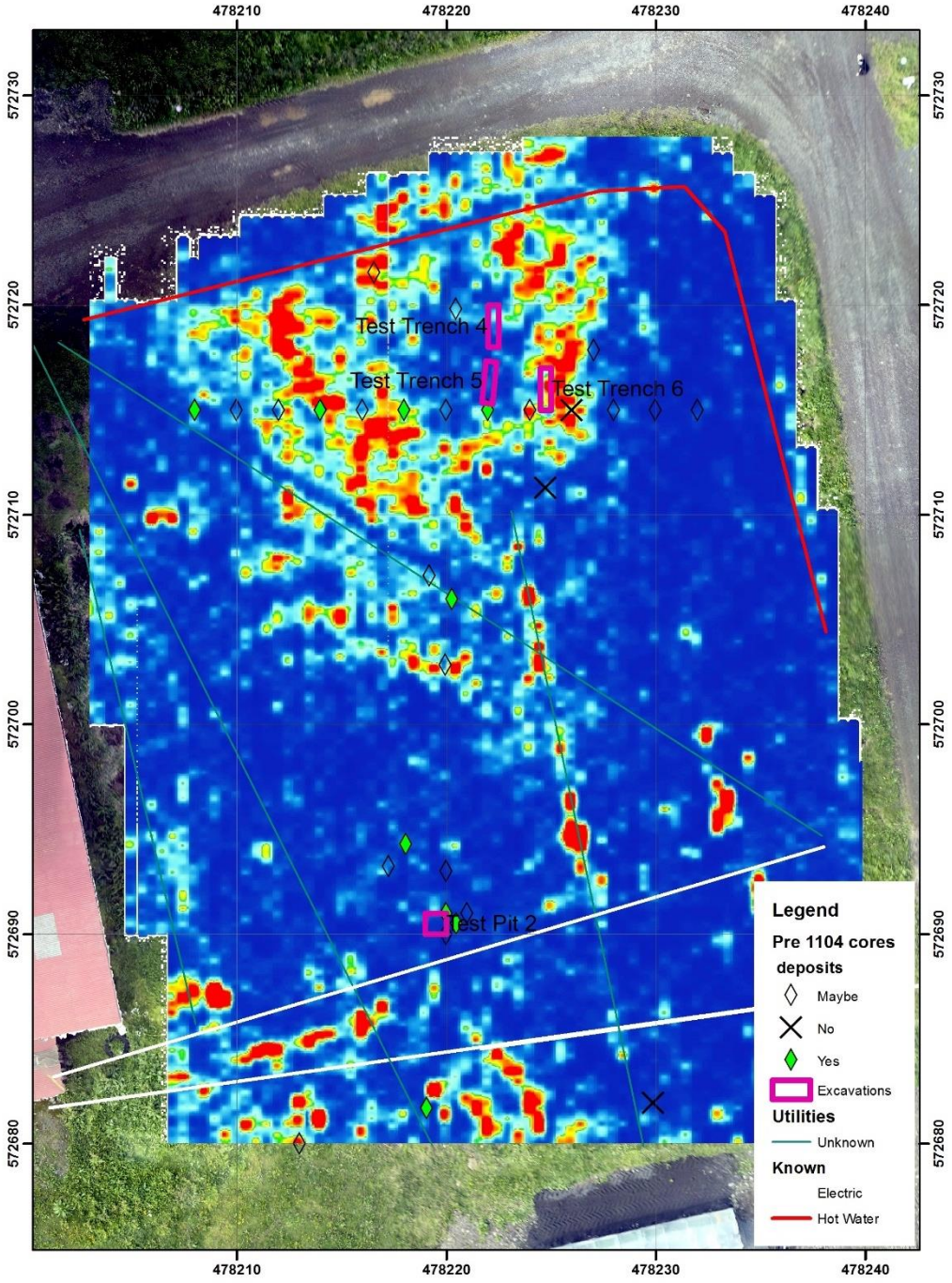

Figure 17. 3 GPR slice from 55 cm bgs with cores superimposed.

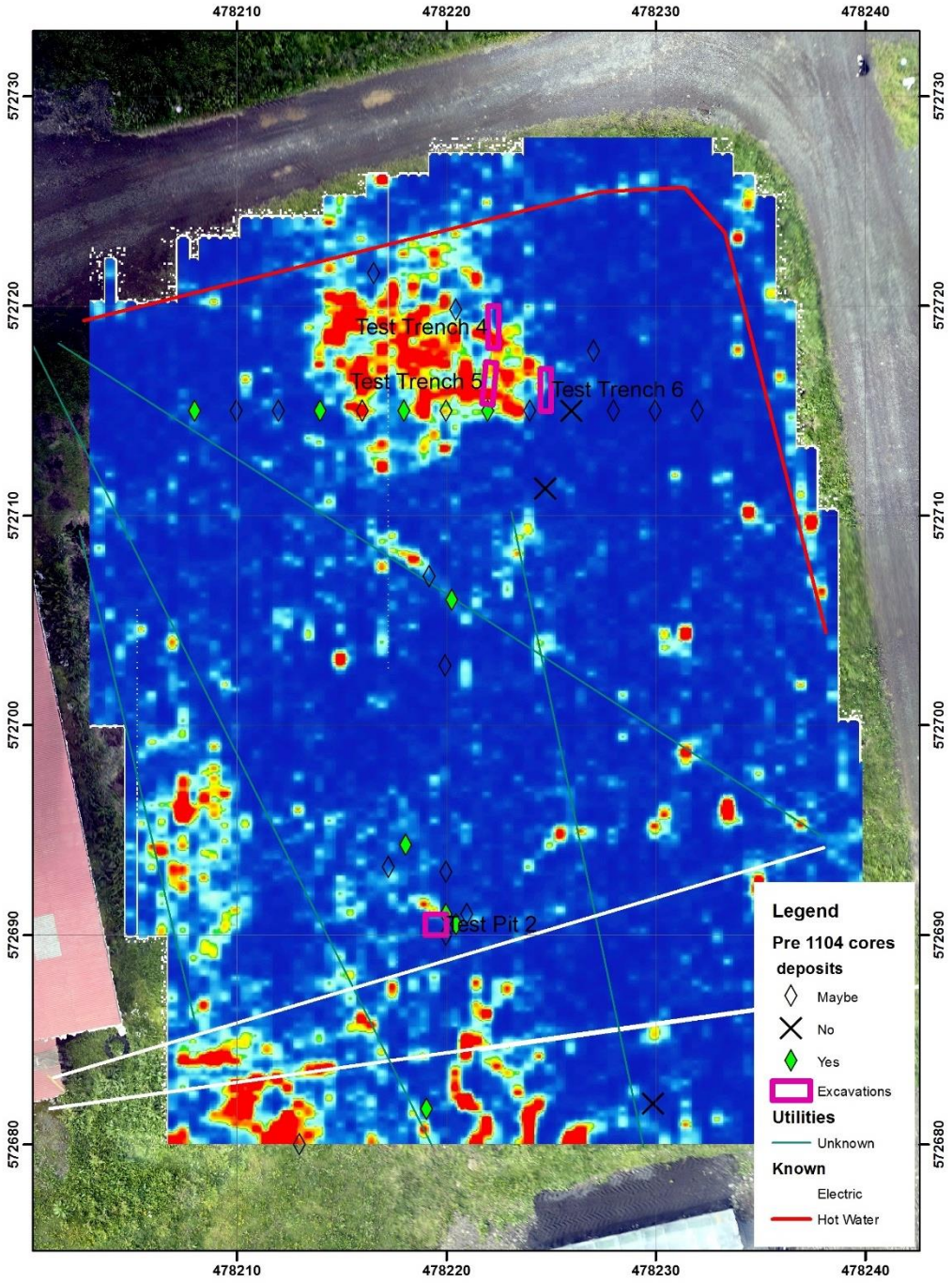

Figure 18. 3 GPR slice from 65 cm bgs with cores and excavations superimposed.

5.0 TEST EXCAVATIONS

Three hand excavated test pits (1, 2, & 3) and one machine dug test trench (5) were completely excavated at the main farm mound at Egg (Place 0). Test trench 4 & 6 were not

completed . These interventions suggest a complex, large and varied cultural landscape at Egg.

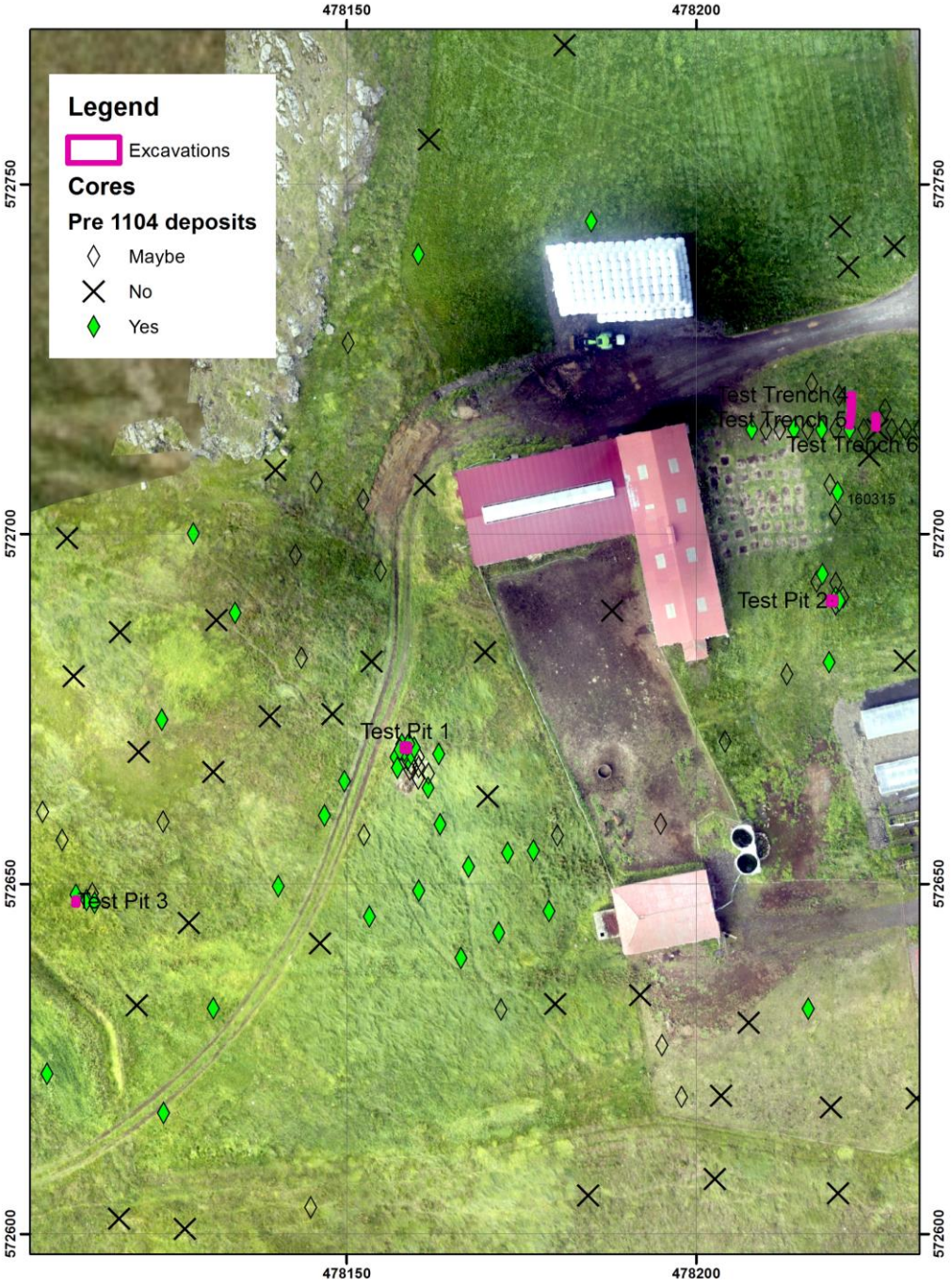

Figure 19. Test pit locations with Kite photograph and pre 1104 core results

5.1.1 Test pits

Three test pits were excavated with shovel and trowel. Test pit 1 is the most complicated sequence, and probably the earliest cultural deposits exposed by the 2016 excavations. It was placed based on the results of a number of cores, many of which presented excellent tephra

preservation (Figure 20). The area is on a west facing slope and many of the cores in the area of test pit 1 also presented substantial midden deposits (see Figure 6, Figure 10, & Figure 11) suggesting the area was part of an extensive early midden. Deposits below the H1 tephra were screened through ¼ in mesh and paleoethnobotanical samples were taken from each context. The 1300 tephra was identified neither during excavation nor in the profile, but [101] and [102] seemed to be relatively intact and showed no disturbance. That being said, both of these contexts showed little cultural activity. Below the 1104 and mostly below the very few patches of the 1000 tephra, the LDC deposits of [103] and [104] were marginally more dense with peat ash and bits of charcoal. A series of distinct whitish deposits, [105], [106], and [107], probably hay or maybe dung was encountered below a distinct but patchy 950 tephra layer (Figure 21). These more extensive deposits rested on charcoal layers [109] and [110] that irregularly covered the entire unit, and seems to be related to a probable charcoal pit [112] identified just below that was dug through the LNS and H3, into a sterile deposit [113] that contains traces of H4. There were some traces of a LNS with a thin aeolian deposit between it and the charcoal layer suggesting that this deposit is a little after the LNS but well before the 950 tephra was laid down. The test pit, while containing substantial and early deposits, does hint that the area may not have been used continuously. Specifically, that the area may not have been used immediately before or after the H1 tephra fell, and more importantly hinting that the site could have been abandoned around this time. However, given the results of test pit 2, it is more likely that this specific area of the midden may have fallen out of use.

Figure 20. location of test pit 1 superimposed on kite photograph with tephra from coring displayed.

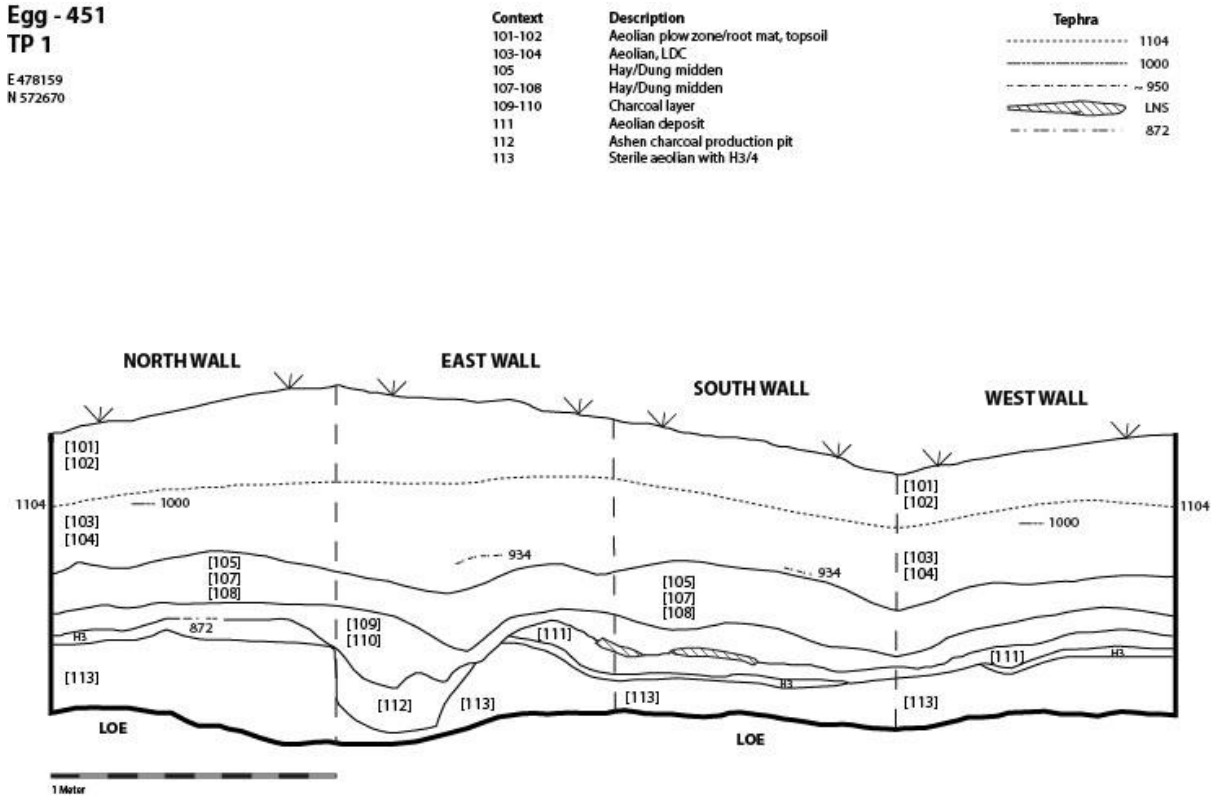

Figure 21. Test pit 1 profile

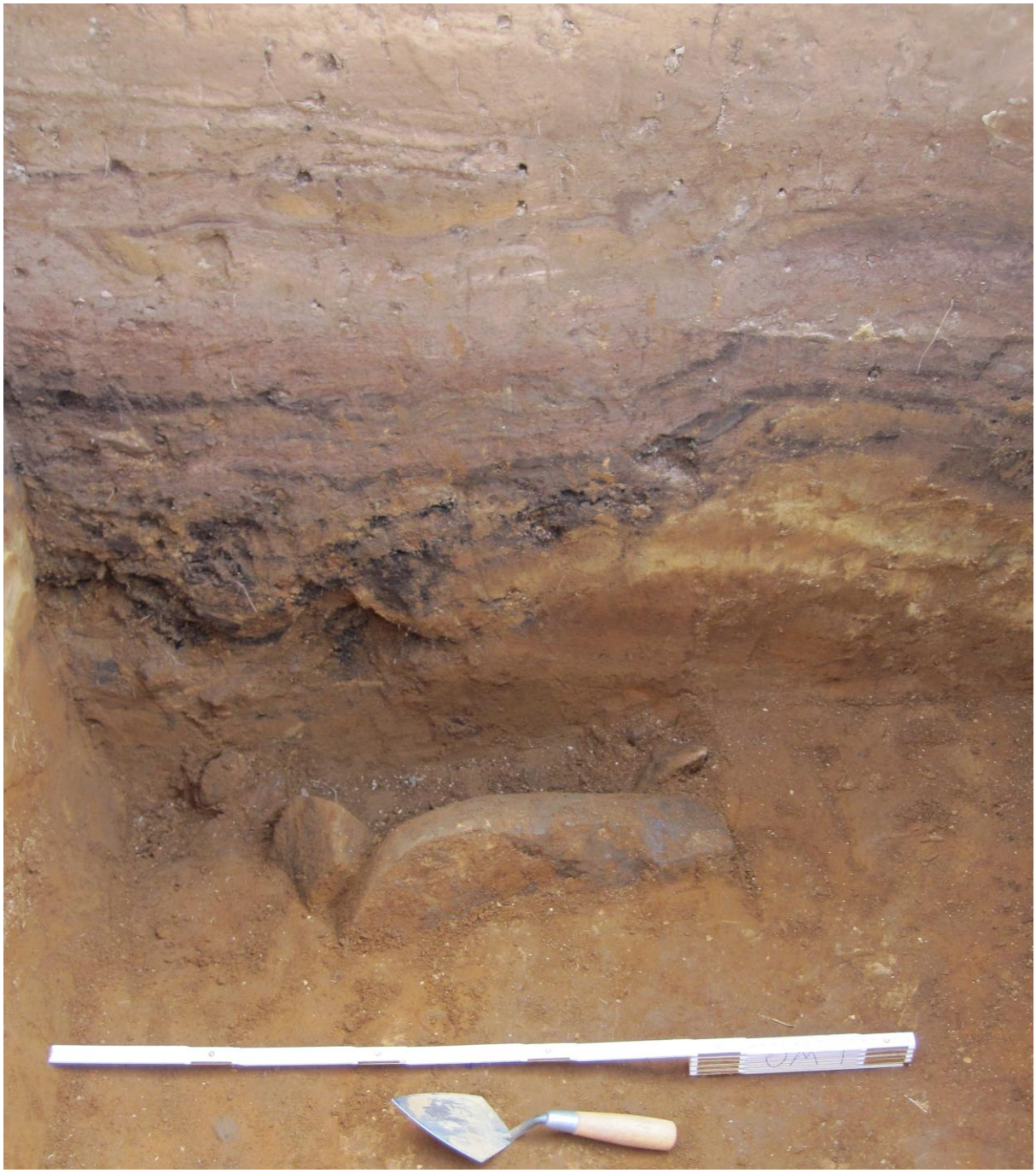

Figure 22. Photo of east wall of Test Pit 1

Test pit 2 was placed based on cores in the area that suggested a different date and nature of midden deposit than presented in test pit 1. Specifically, the early cores in this area (160779 &160950, Figure 23) suggested a sequence that seemed to be associated with cultural deposits that were both immediately before and after the H1 teprha; a different sequence than seen in test pit 1. Thus, a series of further cores were taken to place a second test pit in the

area to assess the potential for site abandonment. In this case under the root mat was a layer of compact gravel [113] that overlaid a pink peat ash deposit [114] and a very compact pink peat ash deposit [115] below that. Both of these ash deposits were on top of a distinct, but not continuous 1300 tephra layer. Deposits below the 1300 tephra were screened through ¼ in mesh and paleoethnobotanical samples were taken from each context. Between the 1300 and the 1104 tephras was a peat ash layer [116]. The H1 in [117] & [118] was heavily thufurized (Feuillet, et al. 2012) in the north-east part of the unit (depicted in the north wall of Figure 24). That being said, [117] & [118] did contain some clear turf inclusions, which casts some doubt on the in situ nature of that tephra layer. However, in the east, the H1 tephra was intact and clearly above the [119] peat ash deposit. Most of the [120] peat ash layer is above the 1000 tephra while most of [121] is below that tephra, but because the 1000 layer was so patchy, the division was not always consistent. There is a small patch of peat ash [123] in an otherwise sterile aeolian deposit [122]. This small patch is the main evidence for activity earlier than the 950 tephra in this location. The sterile [122] overlays a very distinct landnam sequence with a distinct black tephra at the bottom. The H3 tephra was identified at the very bottom of the excavation (Figure 25). Test pit 2 suggests a more continues occupation of Egg, albeit mostly later, than test pit 1. It may be that ash deposition shifted east from the downslope area of test pit 1 to the central portion of the north-south ridge (from which Egg probably gets its name) around test pit 2.

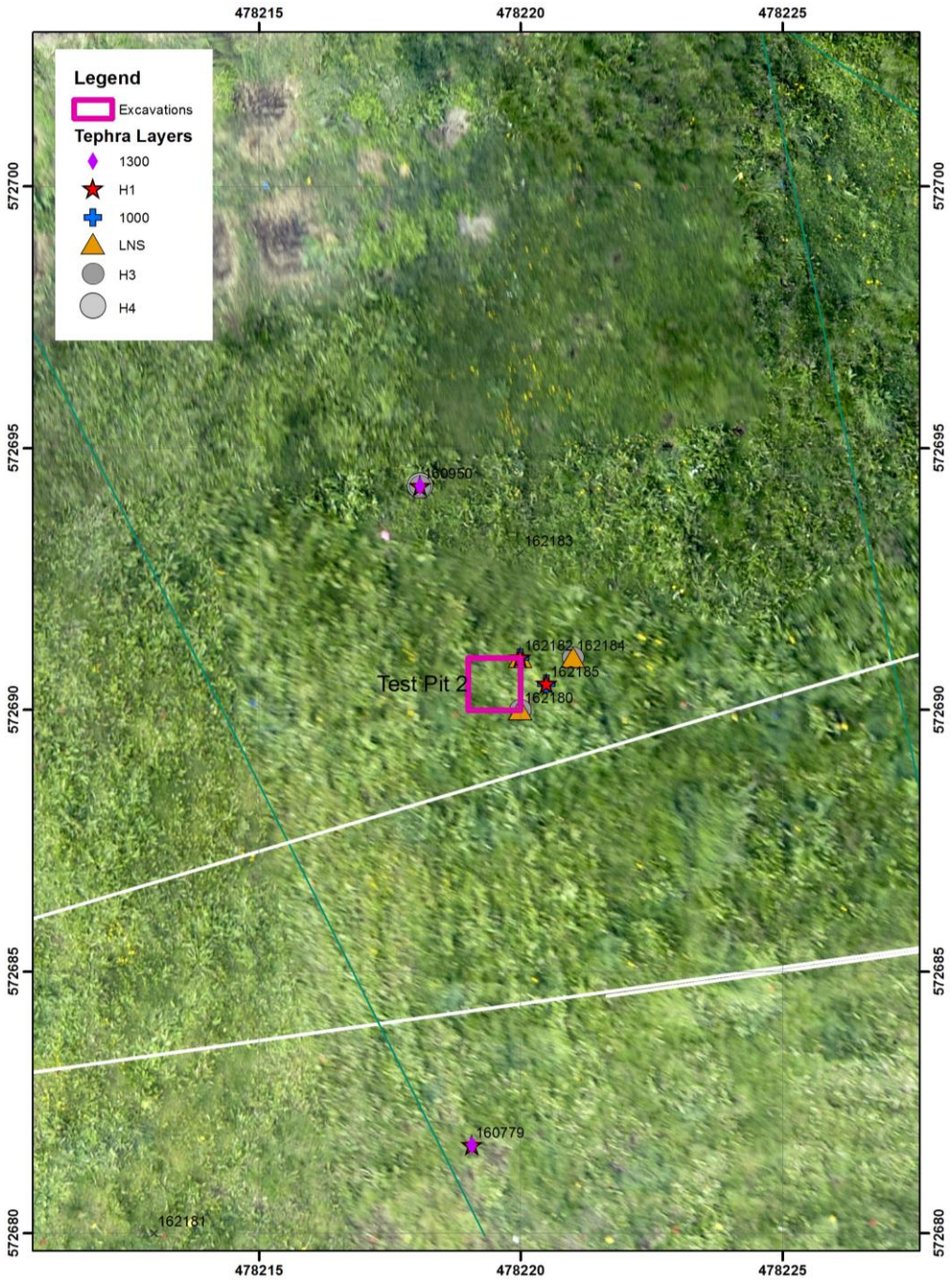

Figure 23. location of test pit 2 superimposed on kite photograph with tephra from coring displayed.

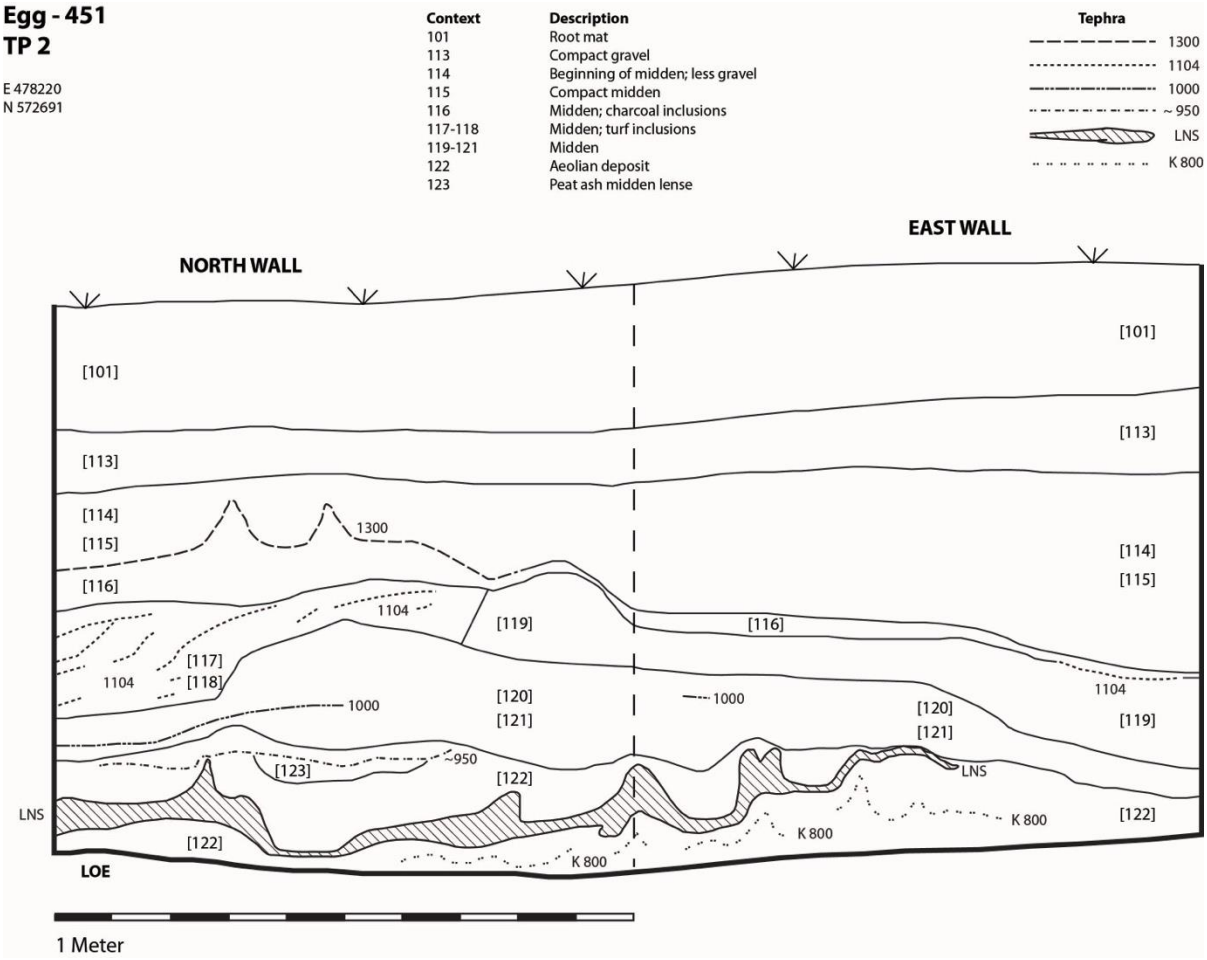

Figure 24. Profile of north and east walls of test pit 2.

Figure 25. Photo of North wall of test pit 2

Test pit 3 was excavated to determine if paleoethnobotanical preservation is substantially different in wetter environments. The sequence is largely consistent with TP1, except there is almost no deposition between the 1104 and the 1000 tephra. Test pit 3 probably represents a secondary deposit of ashes that fell at the edge of the farm mound onto wet boggy deposits. The sequence was fully sampled for paleoethnobotanical remains below the 1300 tephra, but was not screened.

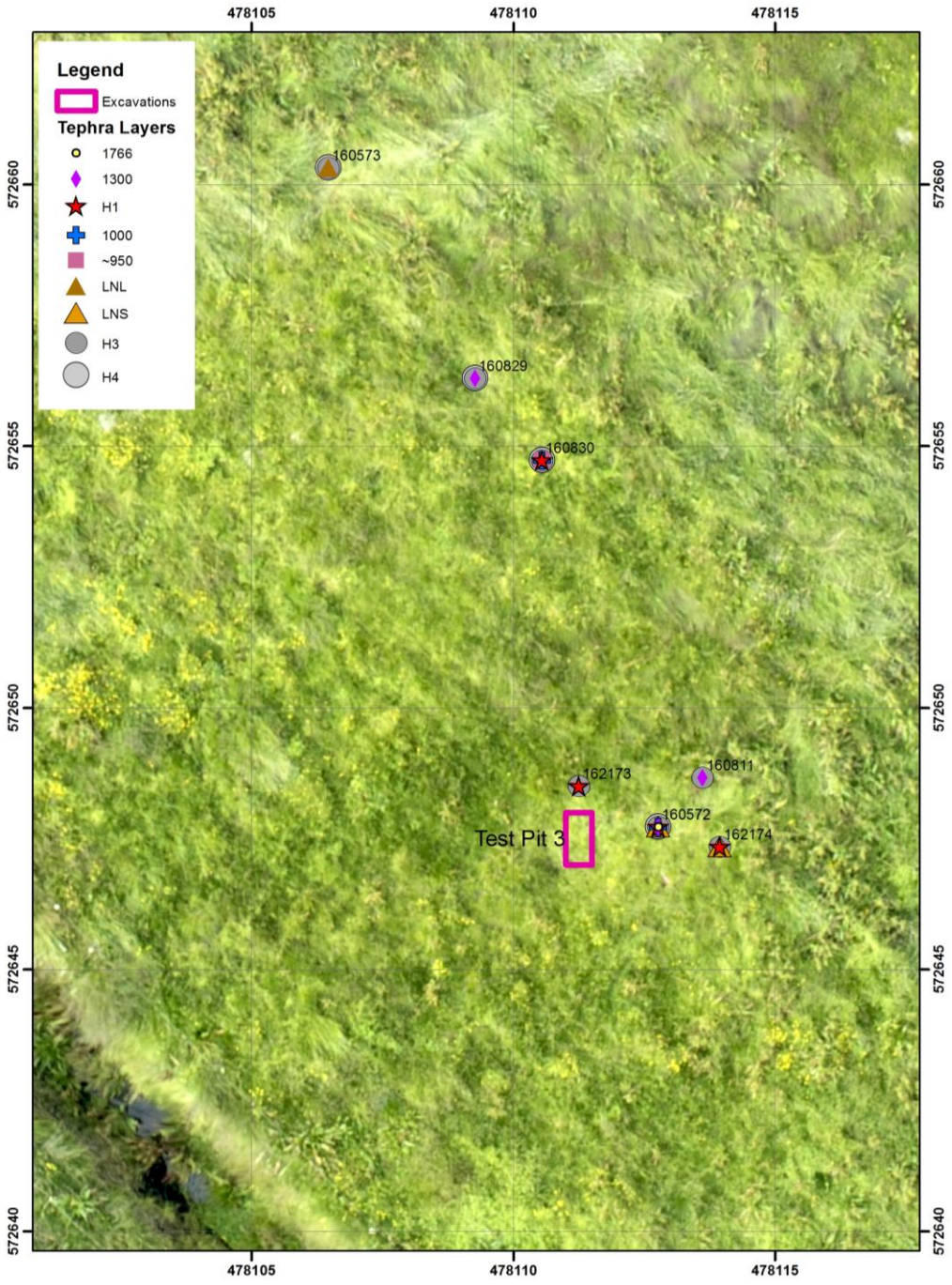

Figure 26. location of test pit 3 superimposed on kite photograph with tephra from coring displayed.

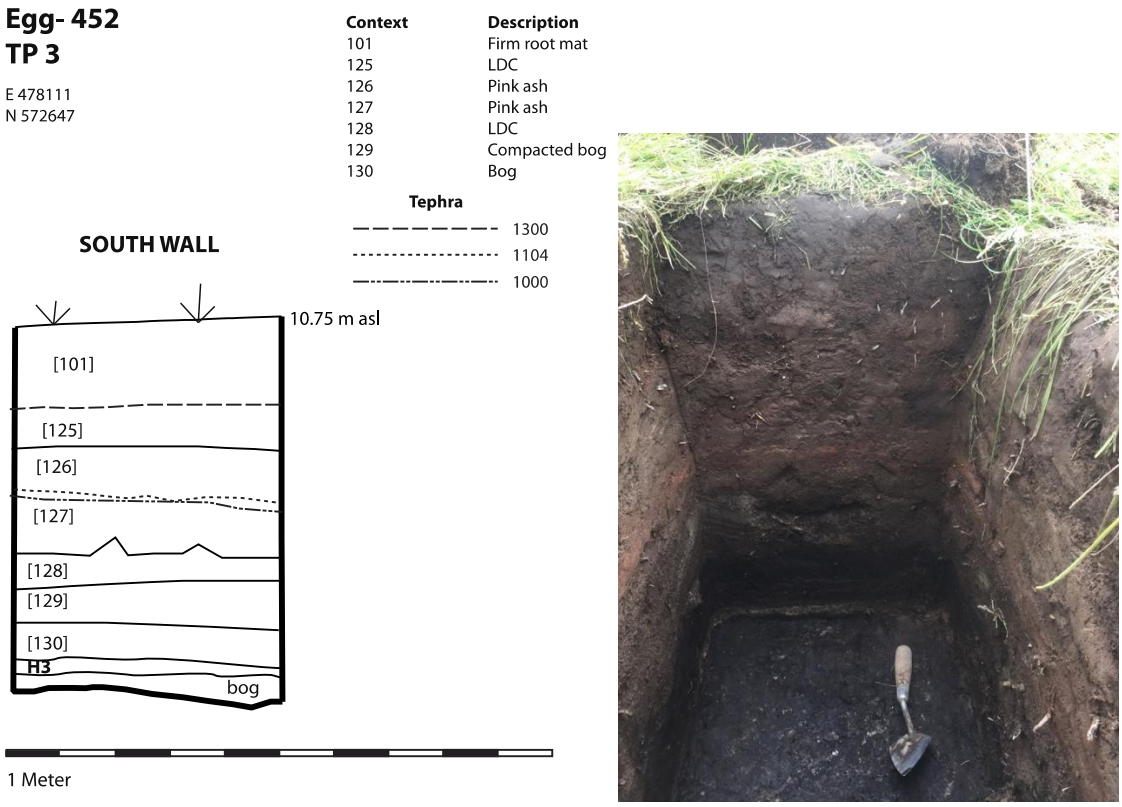

Figure 27. Test pit 3 profile (left) and picture (right)

5.1.2 Test trenches

Test trench 4, 5, and 6 were placed based on the results of coring and geophysics. The trenches were specifically placed to intercept various parts of the "donut" anomaly identified in the GPR (Figure 17) and followed up with a series of cores across the "donut". Test trench 6, was opened, but not excavated. Both Test trench 4 and 5 showed the same sequence. Test trench 4 was excavated by hand, test trench 5 was first excavated by machine and completed by hand. Only test trench 5 was excavated down to the top of the H3 deposit. Most importantly all the test trenches confirmed that the 'donut' anomaly was not part of a churchyard but stony fill on top of a boggy and clayey deposit.

Test trench 5 presented 50 cm of disturbed stony soil [131] with some cultural inclusions immediately below the [101] root mat. The disturbed [131] deposit was identified in the cores as possible grave fill, but it is clearly a continuous layer and the anomaly identified in this area in the GPR is probably the [131]-[132] interface. The [132] turf deposit may be structural, but it is likely a natural deposit, that was probably cut at various times in the past. This turf deposit, which is mixed with a very low level of cultural material, is on top of a clay

deposit [133] which appears to be mostly, but not entirely, sterile. Below the clay layer is another thin, distinct bog layer [134] which is on top of the common reddish subsoil [135] with rocks underneath. The rocks appear to be imbedded in a mixed H3/H4 layer, but it could be a leached soil.

Figure 28. location of test trenches (4, 5, & 6) superimposed on kite photograph with tephra from coring displayed.

Figure 29. Davíð Logi Jónsson uses his tractor to excavate test trench 5 while Brian Damiata and Aileen Balasalle look on.

This sequence suggests that that area of the "donut" anomaly may have been a depression in the past, and was potentially much wetter than it is today. The area does not appear to contain substantial structural remains, and almost surely not those of a churchyard.

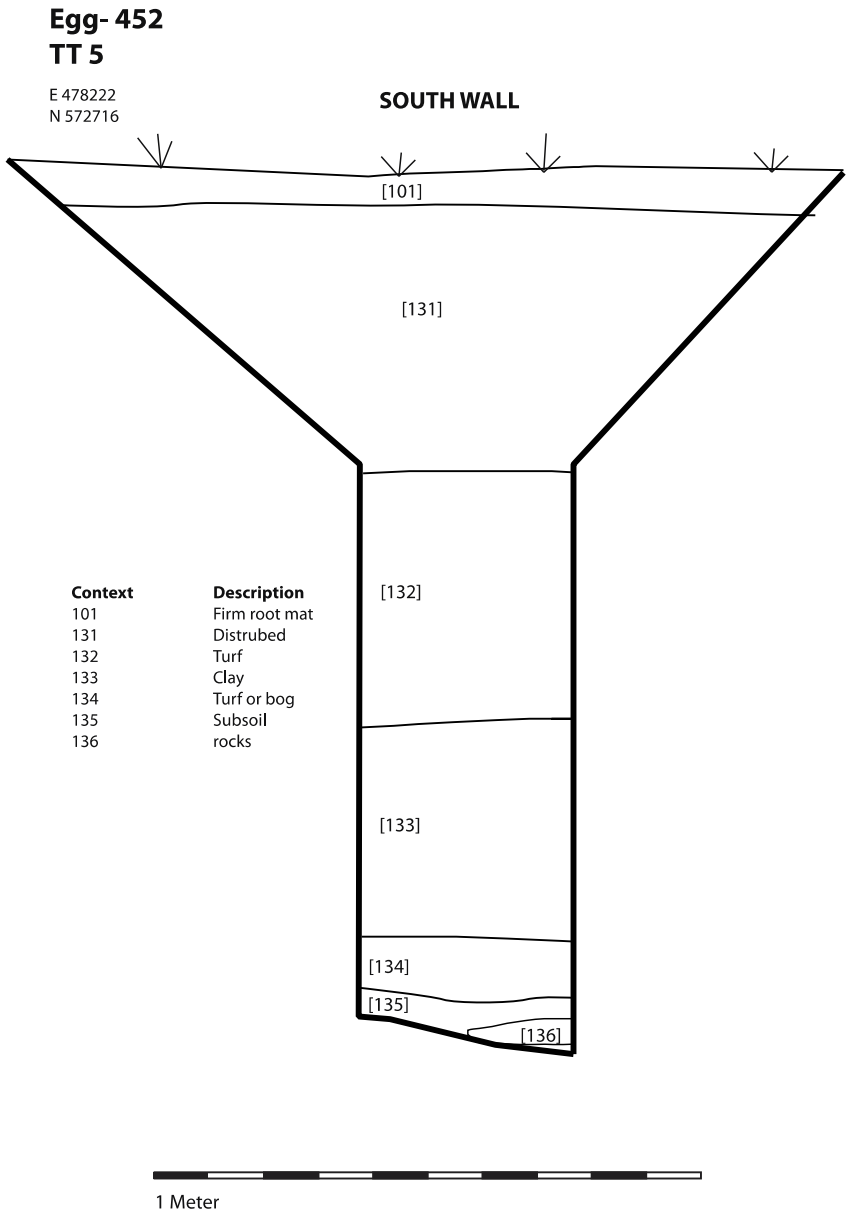

Figure 30. Profile of south wall of Test Trench 5

Figure 31. Photo of south wall of Test Trench 5.

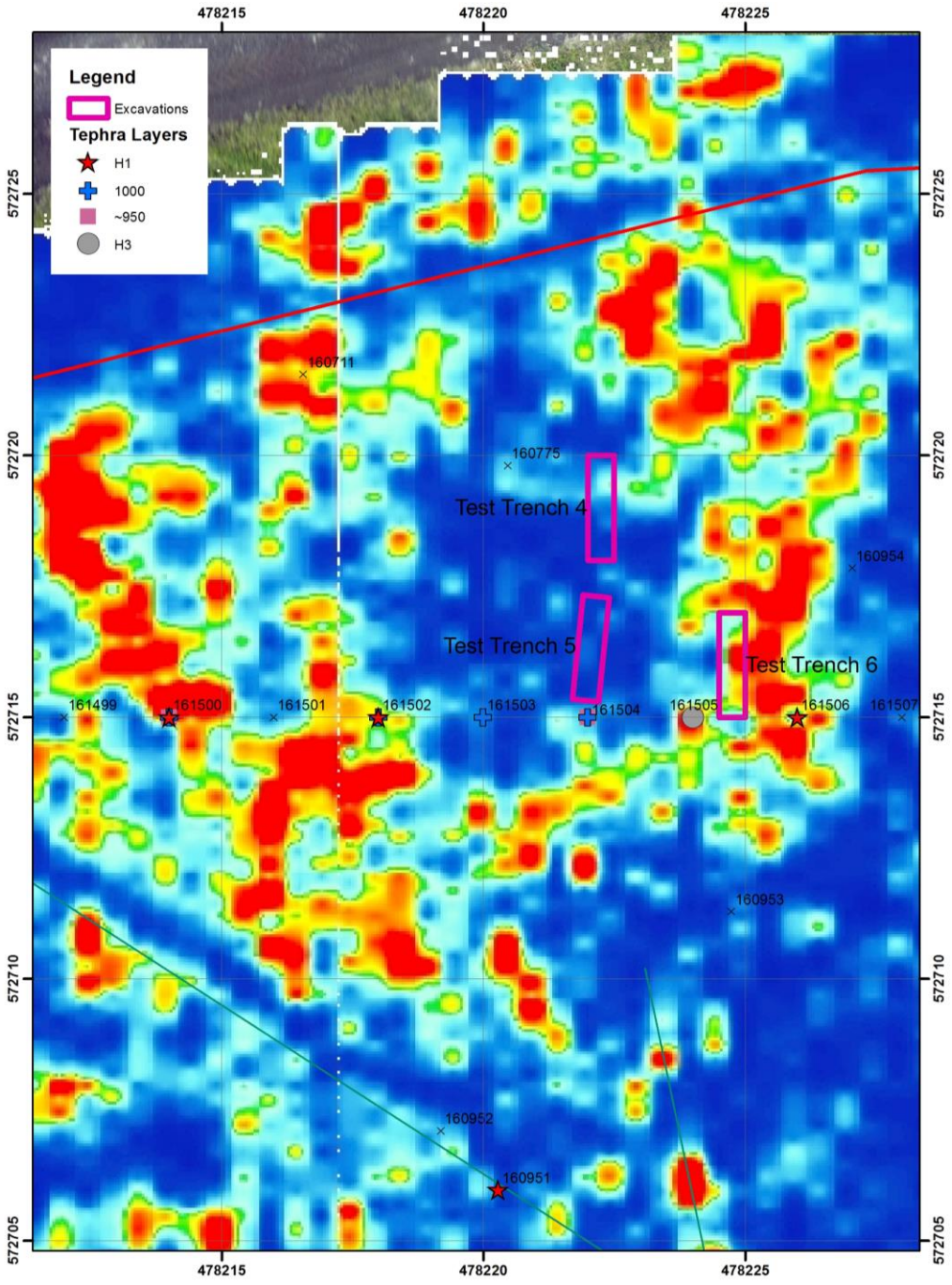

Figure 32.location of test pit 1 superimposed on GPR Slice from 55 cm bgs. with tephra from coring displayed.

6.0 SUMMARY AND CONCLUSIONS

Egg is a complex and early farmstead. The Viking Age component covers a substantial area around the current farm (Figure 33). On the western side of the cow and horse barns (centered on 478125, 572675) the early deposits are substantial and remarkably well preserved. This is evident not just from the cores, but test pit 1 has very little deposit above the 1104 tephra layer and no sign of post 1300 deposits. This well preserved early deposit extends into the area of test pit 3.

In many of the test pits, the Vj~1000 is very close to the H1, usually just a few cm below (e.g., TP1 TP 2, & TP 3). If this interval is an indicator of activity, it may mean that at Egg, saw a lull at this time, but not complete abandonment. Conversely, there is them substantial cultural material between the Vj~1000 and the ~950 tephra and in TP 1, substantial cultural material between the ~950 and the LNL tephras, suggesting intense early activity. Clearly more work is necessary to understand this sequence.

The area between the cow and horse barns (487180, 572670) may contain substantial deposits from all time periods. Because of numerous rocks, this area was only cursorily investigated. This is also true for the area east of the horse barn and north of the living house (478220, 572660), but this area is substantially less likely to overlay areas of earlier activity.

The area east of the current cow barn (478220, 572700) has been intensively investigated with two different geophysical surveys, almost 30 cores, and test trenches. Based on the deposits in test trench 5, as well as surrounding cores and test pits, it would appear that some of this area is overlain by over half a meter of disturbed soil. Below this another half meter of turf and clay deposits, mostly devoid of artifacts. There are plans to build a modern barn east of the current cow barn. We believe that the northern part of this area has been fully investigated and while construction will disturb and destroy archaeological deposits, the sequence and deposit types have been recorded. In the southern part of this area, near test pit 2, both that excavation and the GPR suggest that there are intact cultural deposits that should be monitored during excavation for construction.

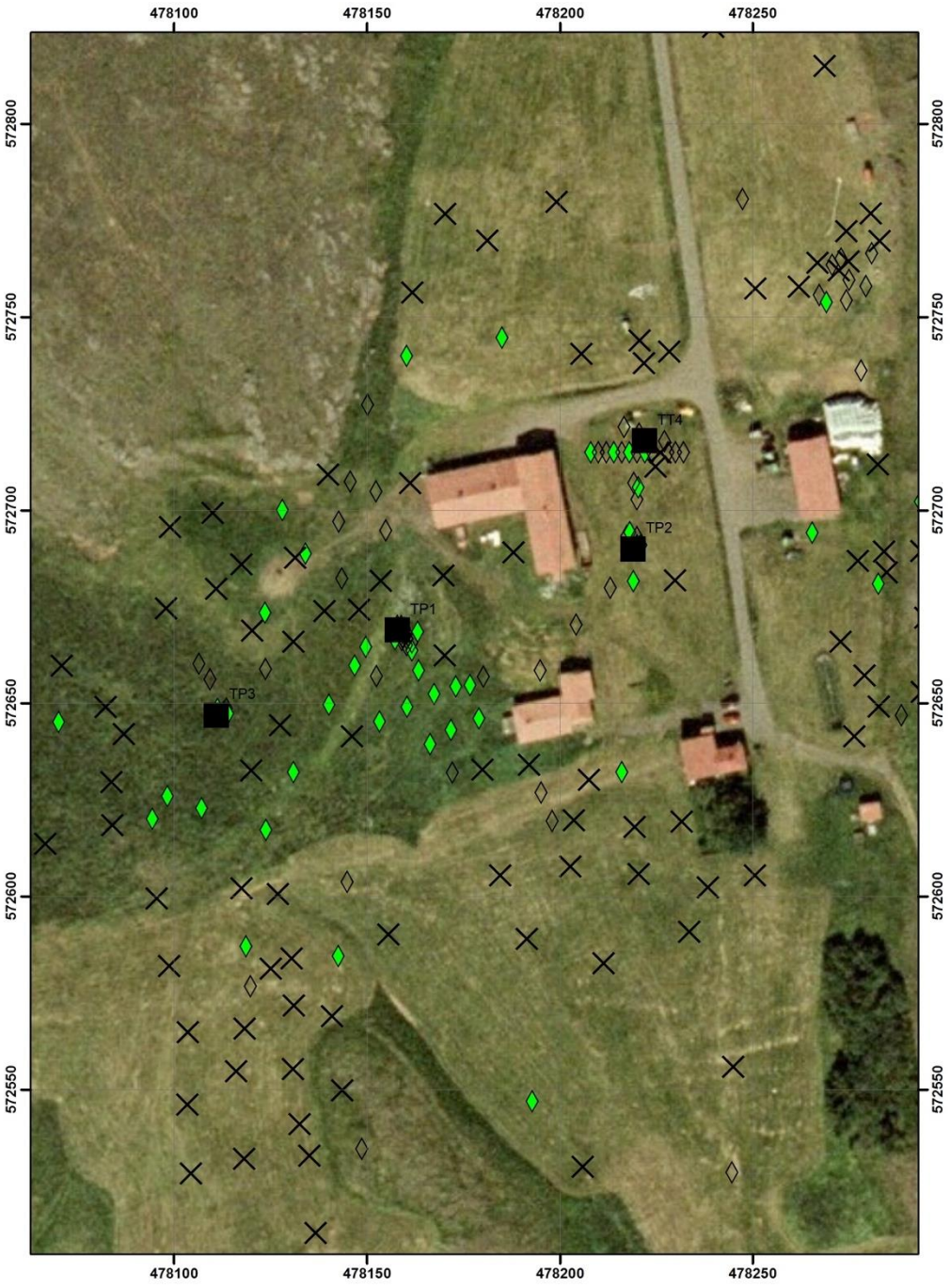

Figure 33. Overview of archaeological work at Egg

7.0 REFERENCES

Arnalds, Ólafur
2004 Volcanic soils of Iceland. *Catena* 56(1-3):3-20.

2008 Soils of Iceland. *Jokull* 58:409-421.

Arnalds, Ólafur, C. T. Hallmark and L. P. Wilding
1995 Andisols from 4 Different Regions of Iceland. *Soil Science Society of America Journal* 59(1):161-169.

Boygle, J.
1999 Variability of tephra in lake and catchment sediments, Svinavatn, Iceland. *Global and Planetary Change* 21(1-3):129-149.

Cossart, Etienne, Denis Mercier, Armelle Decaulne, Thierry Feuillet, Helgi Páll Jónsson and Þorsteinn Saemundsson
2014 Impacts of post-glacial rebound on landslide spatial distribution at a regional scale in northern Iceland (Skagafjörður). *Earth Surface Processes and Landforms* 39(3):336-350.

Davies, S. M., G. Larsen, S. Wastegard, C. S. M. Turney, V. A. Hall, L. Coyle and T. Thordarson
2010 Widespread dispersal of Icelandic tephra: how does the Eyjafjoll eruption of 2010 compare to past Icelandic events? *Journal of Quaternary Science* 25(5):605-611.

Dugmore, Andrew J and Anthony J Newton
2012 Isochrons and beyond: maximising the use of tephrochronology in geomorphology. *Jökull* 62:39-52.

Dugmore, Andrew J., G. T. Cook, J. S. Shore, A. J. Newton, K. J. Edwards and Gudrún Larsen
1995 Radiocarbon Dating Tephra Layers in Britain and Iceland. *Radiocarbon* 37(2):10.

Eiriksson, J., K. L. Knudsen, H. Haflidason and J. Heinemeier
2000 Chronology of late Holocene climatic events in the northern North Atlantic based on AMS C-14 dates and tephra markers from the volcano Hekla, Iceland. *Journal of Quaternary Science* 15(6):573-580.

Fei, J. and J. Zhou
2006 The possible climatic impact in China of Iceland's Eldgja eruption inferred from historical sources. *Climatic Change* 76(3-4):443-457.

Feuillet, T., D. Mercier, A. Decaulne and E. Cossart
2012 Classification of sorted patterned ground areas based on their environmental characteristics (Skagafjorour, Northern Iceland). *Geomorphology* 139:577-587.

Gaffney, Chris and John Gater
2003 *Revealing the buried past : geophysics for archaeologists*. Tempus, Stroud.

Goodman, D., Y. Nishimura and J.D. Rogers
1995 GPR time slices in archaeological prospection. *Archaeological Prospection* 2:85-89.

Goodman, D., S Piro, Y Nishimura, K Schneider, H. Hongo, N. Higashi, J Steinberg and B. Damiata
2008 GPR Archaeometry. In *Ground Penetrating Radar Theory and Applications*, edited by H. Jol, pp. 479-508. Elsvier, New York.

Goodman, D., J Steinberg, B. Damiata, Y Nishimura, S Piro and K Schneider
2007 GPR Imaging of Archaeological Sites. In *Reconstructing Human-Landscape Interactions, Dig 2005 Conference, Developing International Geoarchaeology*, edited by L. Wilson, P. Dickinson and J. Jeandron, pp. 202-217. Cambridge Scholars Publishing, Cambridge.

Grönvold, K., N. Óskarsson, S. J. Johnsen, H. B. Clausen, C. U. Hammer, G. Bond and E. Bard
1995 Ash layers from Iceland in the Greenland GRIP ice core correlated with oceanic and land sediments. *Earth and Planetary Science Letters* 135:149-155.

Hallsdóttir, M.
1987 Pollen analytical studies of human influence on vegetation in relation to the Landnám tephra layer in Southwest Iceland. Ph.D., Department of Quarternary Geology, Lund University, Lund.

Hammer, Claus U, Henrik B Clausen and Willi Dansgaard
1980 Greenland ice sheet evidence of post-glacial volcanism and its climatic impact. *Nature* 288:230-235.

Hið íslenska Bókmenntafélag
1858 *Biskupa Sögur* S.L. Møller, Copenhagen.

Johnsen, Jón
1847 *Jarðatal á Íslandi*. S. Trier, Copenhagen.

Larsen, Gudrún
1984 Recent volcanic history of the Veidivotn fissure swarm, southern Iceland -- an approach to volcanic risk assessment. *Journal of Volcanology and Geothermal Research* 22(1-2):33-58.

Larsen, Gudrún, Andrew J. Dugmore and Anthony Newton
1999 Geochemistry of historical-age silicic tephras in Iceland. *The Holocene* 9(4):9.

Larsen, Gudrún, Jón Eiríksson, Karen Louise Knudsen and Jan Heinemeier
2002 Correlation of late Holocene terrestrial and marine tephra markers, north Iceland: implications for reservoir age changes. *Polar research* 21(2):283-290.

Larsen, Gudrún, Anthony J. Newton, Andrew J. Dugmore and E. G. Vilmundardottir
2001 Geochemistry, dispersal, volumes and chronology of Holocene silicic tephra layers from the Katla volcanic system, Iceland. *Journal of Quaternary Science* 16:119-132.

Linford, N.
2006 The application of geophysical methods to archaeological prospection. *Reports on Progress in Physics* 69(7):2205-2257.

Magnússon, Árni and Páll Vídalín
1930 *Járðabók* 9. 13 vols. Hið íslenska fræðafélag, Copenhagen.

Ólafsson, Guðmundur
1985 Gjóskulög í Austurdal og Vesturdal, Skagafirdi. , Námsritgerd við Háskóla Íslands, Reykjavík.

Pálsson, Hjalti
2010 *Byggðasaga Skagafjarðar: V Bindi Rípurhreppur - Viðvíkurhreppur*. Sögufélag Skagafirðinga, Sauðárkróki (Iceland).

Sigurgeirsson, Magnús Á.
1998 Gjóskulagarannsóknir á Hofstoðum 1992–1997. *Archaeologia Islandica* 1:110-118.

Sigurgeirsson, Magnús Á., Ulf Hauptfleisch, Anthony Newton and Árni Einarsson
2013 Dating of the Viking Age Landnám Tephra Sequence in Lake Mývatn Sediment, North Iceland. *Journal of the North Atlantic* 21:1-11.

Sveinbjarnardóttir, Guðrún
1992 *Farm Abandonment in Medieval and Post-Medieval Iceland: an Interdisciplinary Study*. Oxbow Monograph 17. Oxbow Press, Oxford.

Thórarinsson, S.
1967 The eruptions of Hekla in historical times. In *The Eruption of Hekla, 1947-1948. Vol. 1 of The Eruptions of Hekla in Historical Times: A Tephrochronological Study*, edited by S. Thórarinsson, pp. 5-183. Leiftur, Reykjavik.

Thordarson, T., D. J. Miller, G. Larsen, S. Self and H. Sigurdsson
2001 New estimates of sulfur degassing and atmospheric mass-loading by the 934 AD Eldgja eruption, Iceland. *Journal of Volcanology and Geothermal Research* 108(1-4):33-54.

Wastegard, S., V. A. Hall, G. E. Hannon, C. van den Bogaard, J. R. Pilcher, M. A. Sigurgeirsson and M. Hermanns-Audardottir
2003 Rhyolitic tephra horizons in northwestern Europe and Iceland from the AD 700s-800s: a potential alternative for dating first human impact. *Holocene* 13(2):277-283.

Zielinski, Gregory A., Paul A. Mayewski, L. David Meeker, Karl Grönvold, Mark S. Germani, Sallie Whitlow, Mark S. Twickler and Kendrick Taylor
1997 Volcanic aerosol records and tephrochronology of the Summit, Greenland, ice cores. *Journal of Geophysical Research* 102(12):26625-26640.

Þórarinsson, Sigurður
1977 Gjóskulög og gamlar rústir. *Árbók* 1976:5-38.

APPENDIX A – BASIC PRINCIPLES OF FREQUENCY-DOMAIN ELECTROMAGNETICS

The frequency-domain electromagnetic (FDEM) method is an active non-destructive geophysical method that is used to obtain shallow subsurface information. In the EM method, a time-varying magnetic field is generated by driving an alternating current through either a loop of wire or a straight wire that is grounded at both ends. Induced or eddy currents with flow within any conductive solid or fluid material that is present beneath the area of investigation. The eddy currents, in turn, generate their own magnetic fields such that at any point in space, the total magnetic field is the superposition of the primary field due to the source current and secondary fields due to the eddy currents, as schematically illustrated in Figure B1. By discriminating between primary and secondary fields, variations in the EM properties of the ground can be discerned.

EM instruments measure both out-of-phase (quadrature) and in-phase components of the induced magnetic fields. The former is a measure of the bulk apparent ground conductivity; the latter is related to magnetic susceptibility and is particularly sensitive to the presence of metallic objects. Bulk apparent ground conductivity reflects true conductivity when the subsurface is homogeneous and isotropic, which is rarely the case in practice. For heterogeneous conditions, it represents an integrated effect of the all the conductivity within the volume of ground being sensed. It does not, however, represent an average conductivity and in fact can be lower or higher than the lowest or highest subsurface conductivities, respectively. A lateral variation in the components is indicative of lateral changes in properties. The conductivity is particularly sensitive to fluid content and dissolved salts or ions. Accordingly, wet sands, clays and materials with high ion content generally have high bulk apparent ground conductivity; dry sands and crystalline rocks have low bulk apparent ground conductivity.

Ideally, EM surveys are conducted in archaeological investigations to find conductive targets in resistive environments such as middens and rammed-earthed walls. Although more subtle and difficult to detect, resistive targets such as buried stone walls and foundations can also be detected through EM surveying.

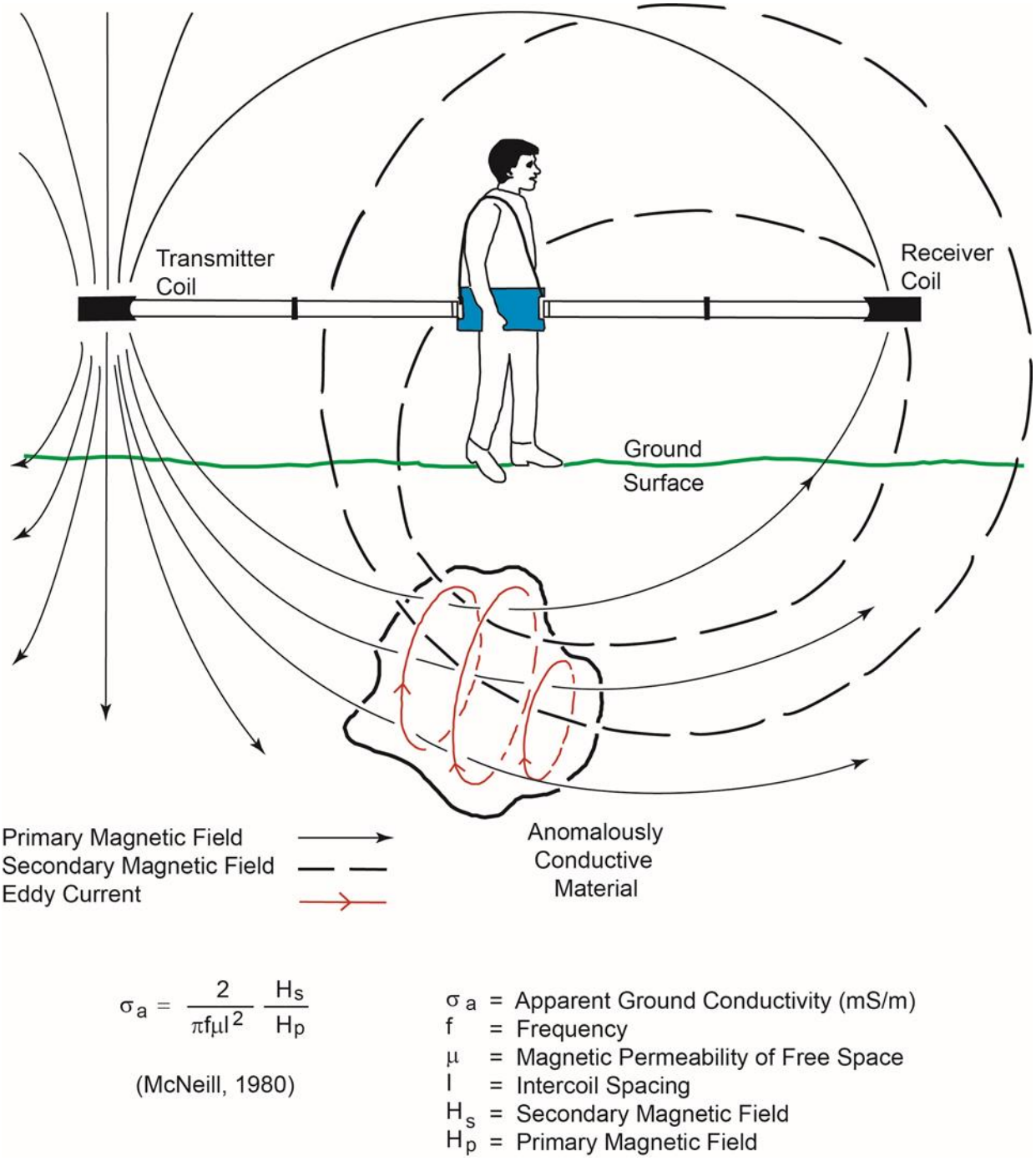

Figure A1. Schematic diagram illustrating the principles of FDEM.

APPENDIX B – BASIC PRINCIPLES OF GROUND PENETRATING RADAR

GPR is an active non-destructive geophysical method that is used to image the shallow subsurface. In GPR, electromagnetic (EM) energy is pulsed through a transmitter antenna that is towed along the ground surface. As the energy travels through the ground and encounters distinct changes in electrical properties—specifically, the relative permittivity (E_R) which is a measure of a material's ability to store electrical energy—a portion is reflected back to the ground surface. It is the two-way travel time of the reflected energy that is recorded by a receiver antenna in the form of a single scan at the given location as schematically illustrated in Figure B1. A two-dimensional radargram is produced by combining all of the scans along a transect. The data from many radargrams can be further combined and horizontally sliced at specified time intervals to provide pseudo-three dimensional plan images that oftentimes are easier to interpret (see accompanying figures).

Of all the available geophysical methods, GPR provides the highest possible resolution for imaging the shallow subsurface. The ability to resolved buried features, however, depends partly on the center frequency of the transmitter antenna. Relatively higher frequencies (e.g., 800 MHz) have greater resolving capabilities but at the expense of less penetrating power as compared to lower frequencies (e.g., 500 MHz). The method works best in electrically resistive conditions such as dry sandy soils. In general, electrically conductive environments can severely attenuate the EM energy. The presence of water with high dissolved solids as well as water-retaining materials such as clay and silt, even in minor amounts, can severely limit the depth of penetration.

The use of GPR should be considered whenever the target of interest provides a distinct contrast in relative permittivity (air: $E_R = 1$, water: $E_R = 81$, dry soil: $E_R = 4\text{-}6$, wet soil: $E_R = 10\text{-}30$; rock/bedrock: $E_R = 5\text{-}8$) as compared to the surroundings and is sufficient in size to be detected. Typical targets include: buried stone walls and foundations, graves, site specific stratigraphy and soil thickness/depth to bedrock.

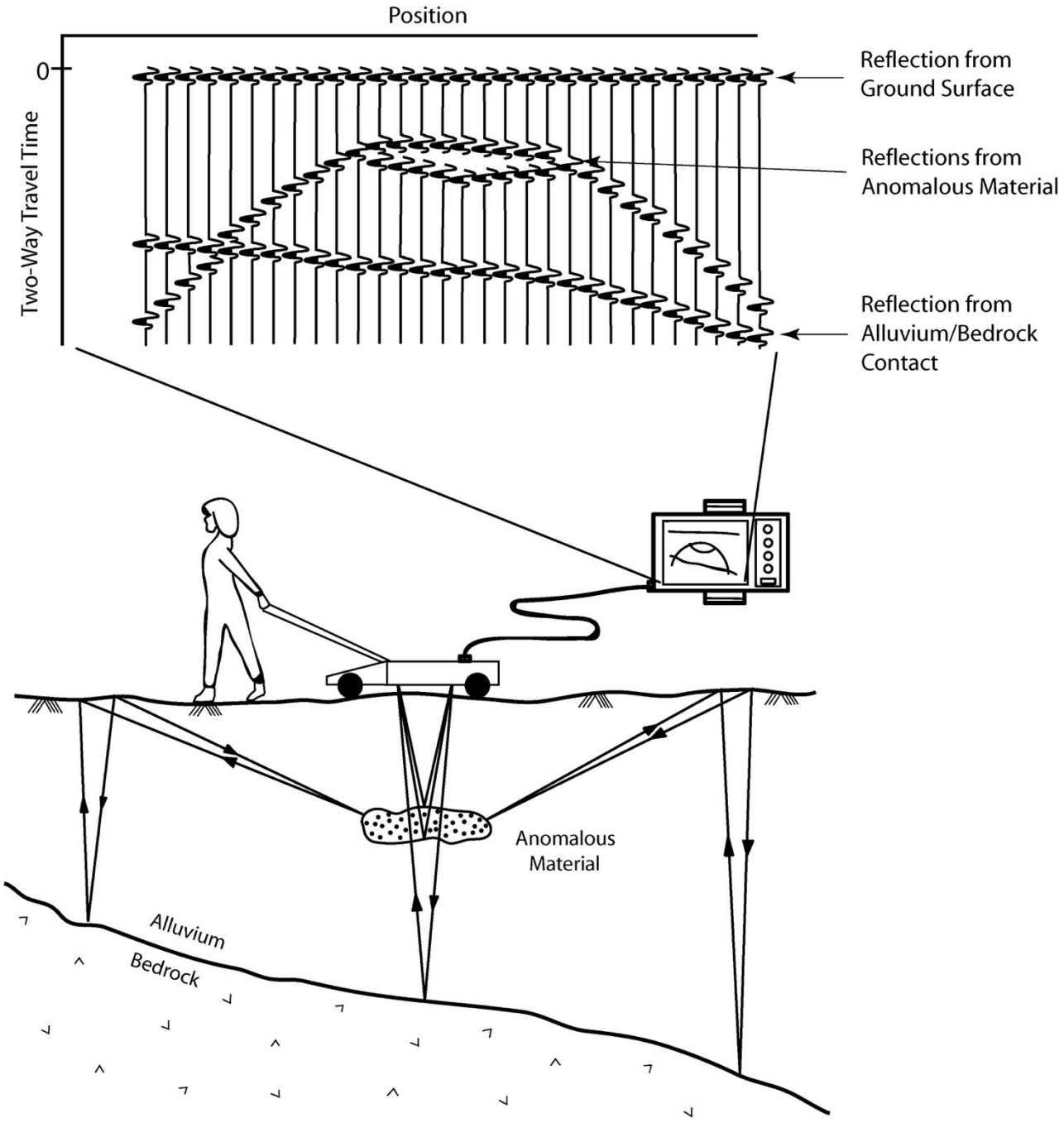

Figure B1. Schematic diagram illustrating the principles of GPR.

APPENDIX C – PLOT OF FDEM DATA

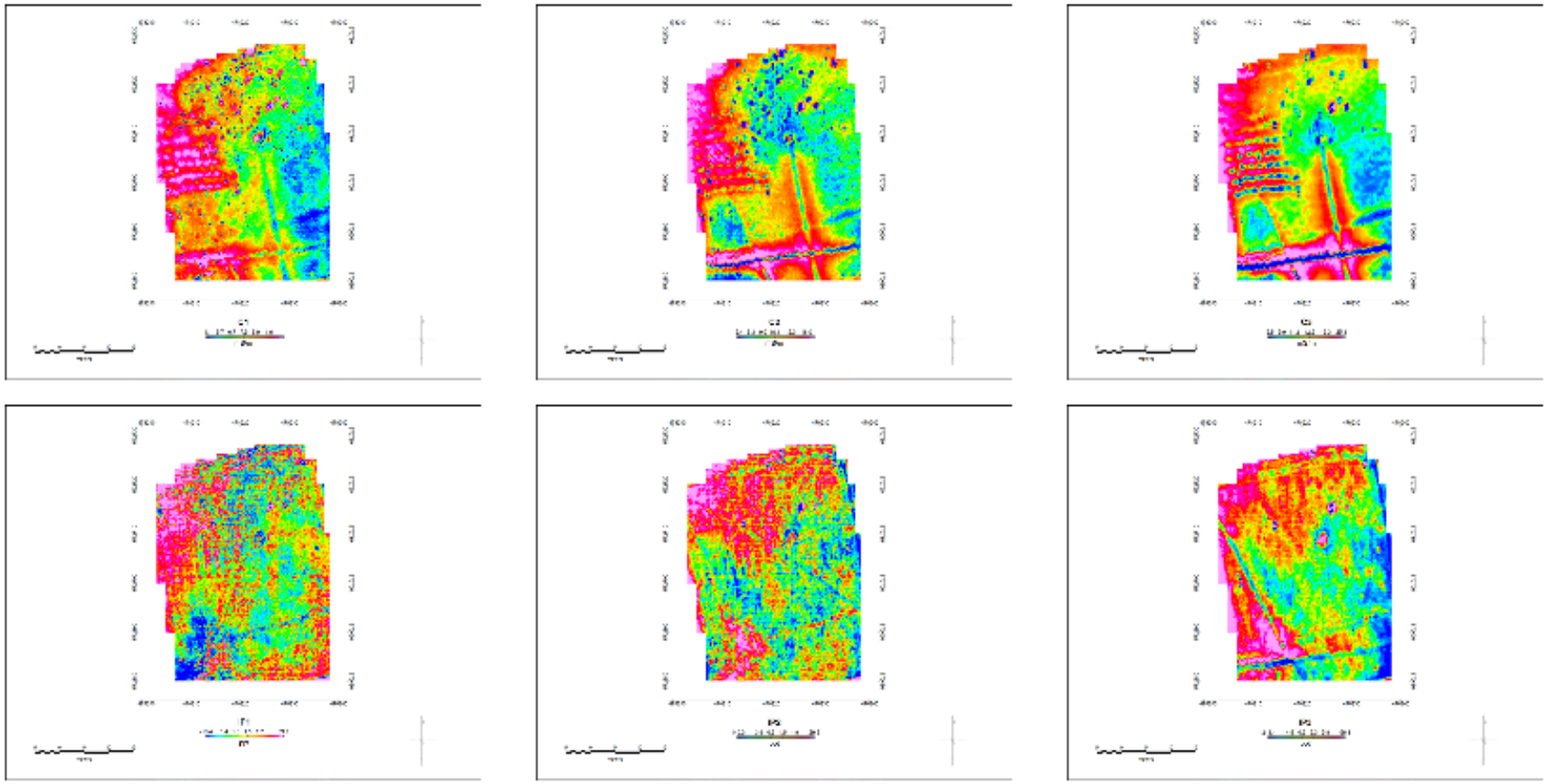

Figure C1. Graphics of all the components of the CMD mini at Egg.

APPENDIX D –RADARGRAMS

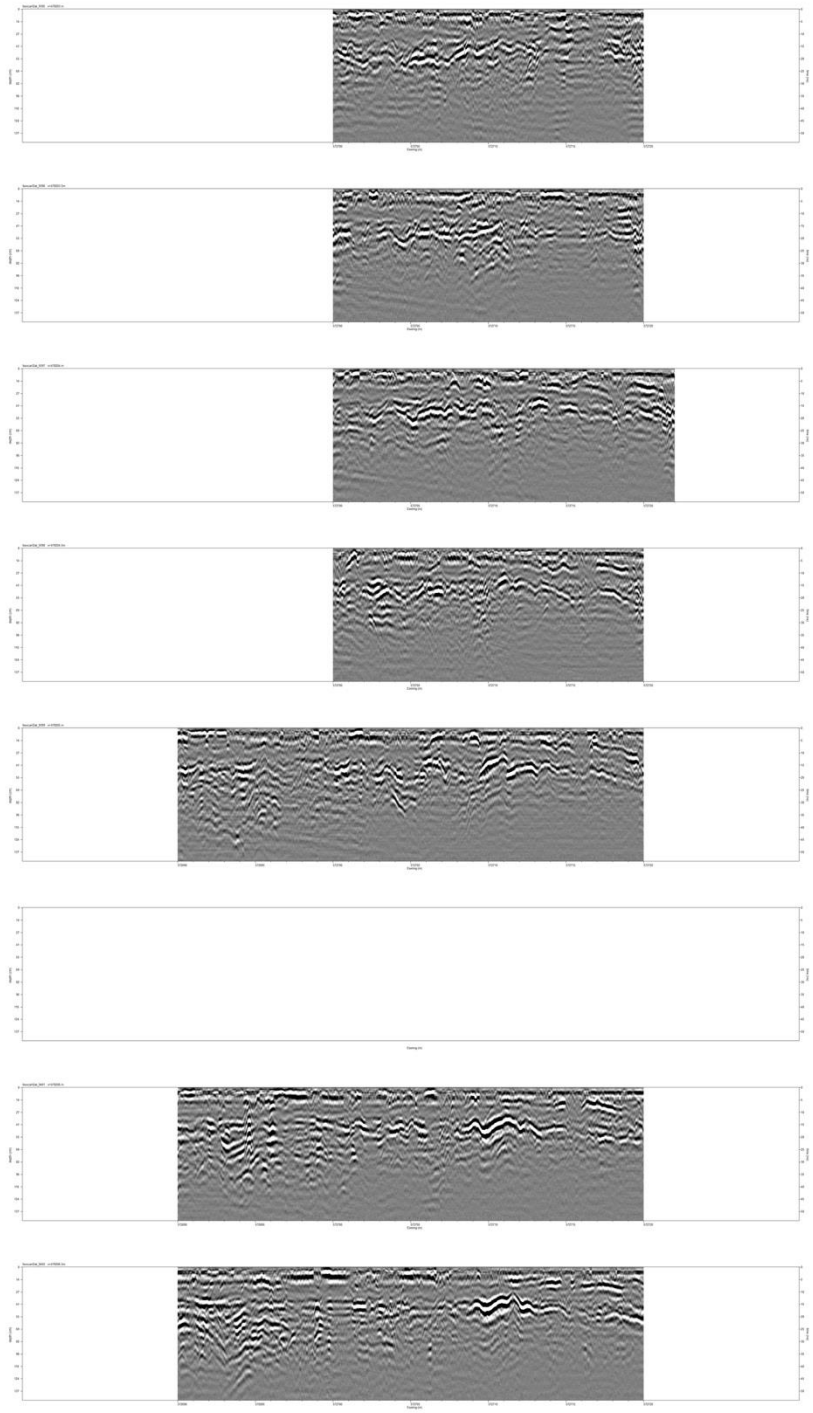

Figure D1. Annotated radargrams for profiles 3995 (478203 E) through 4902 (478206.5E).

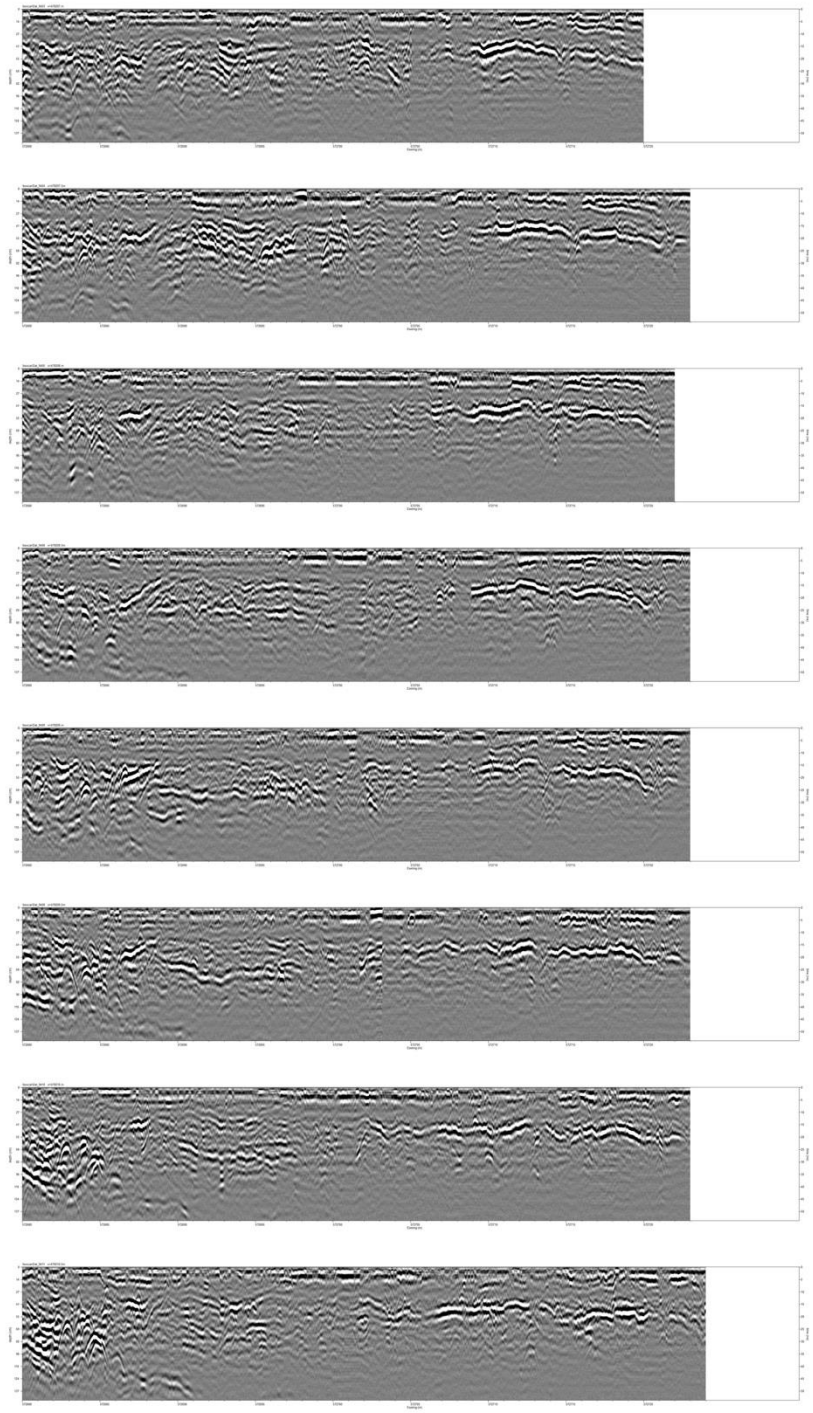

Figure D2. Annotated radargrams for profiles 4903 (478207 E) through 4911 (478210.5E).

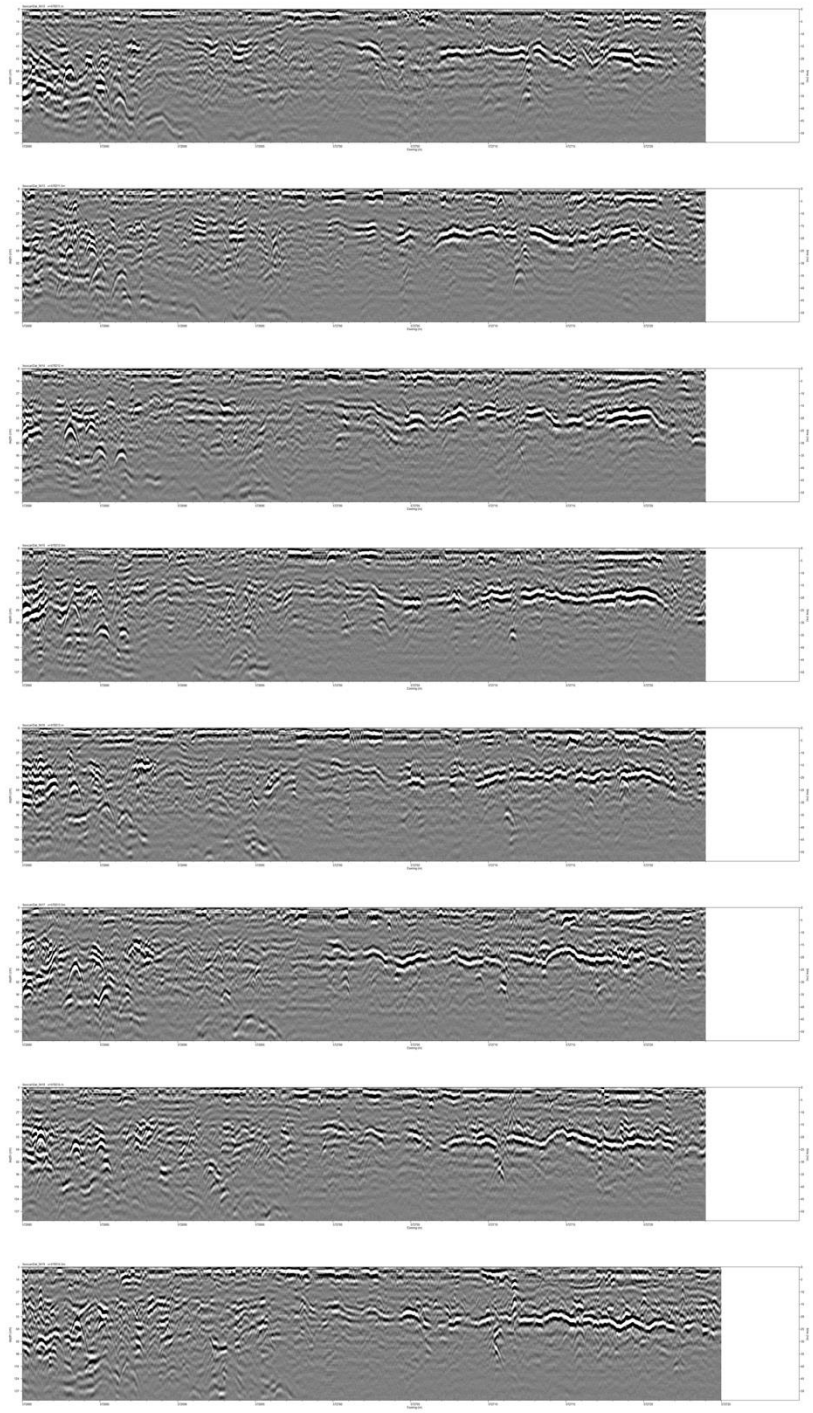

Figure D3. Annotated radargrams for profiles 4912 (478211 E) through 4919 (478214.5E).

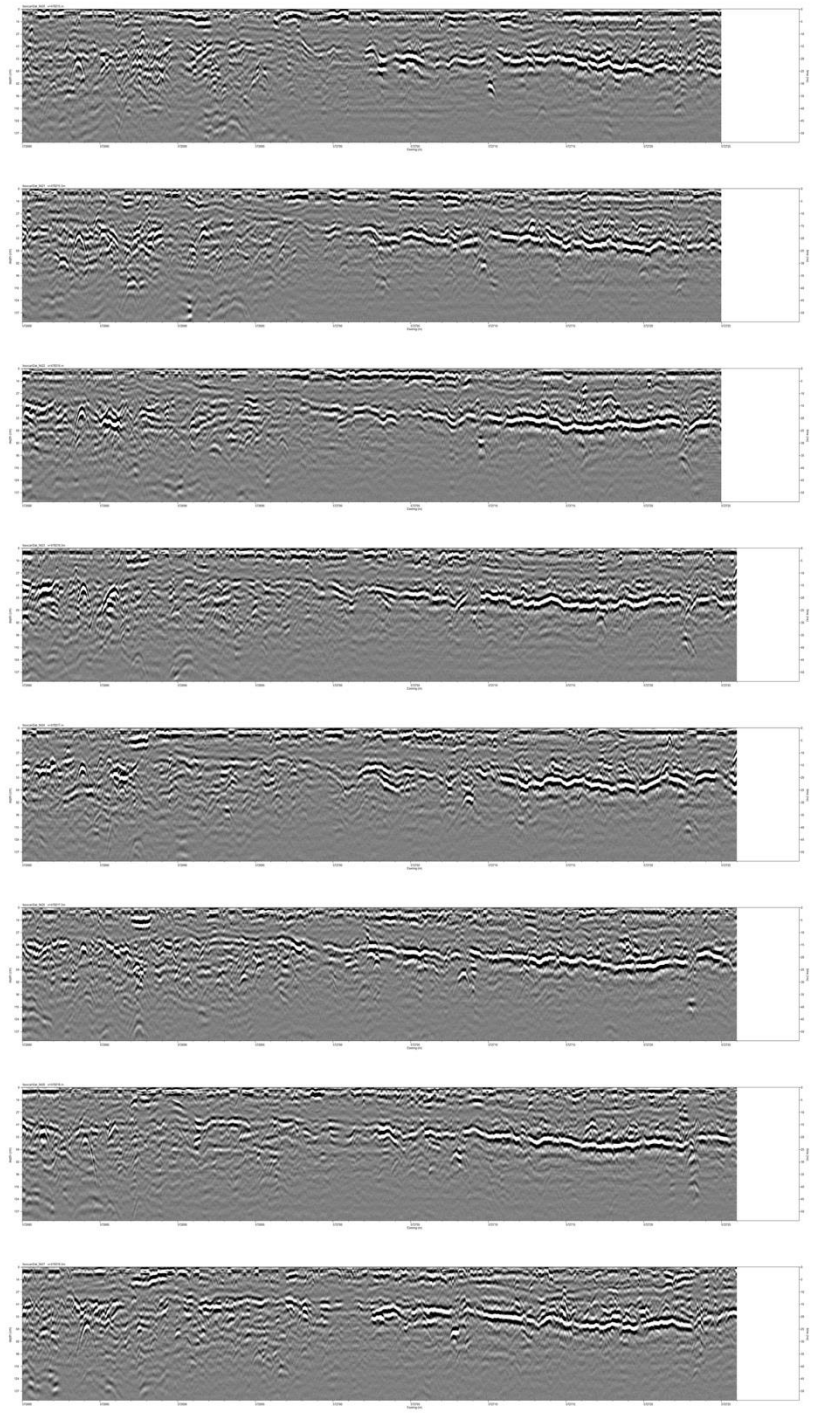

Figure D4. Annotated radargrams for profiles 4920 (478215 E) through 4927 (478218.5E).

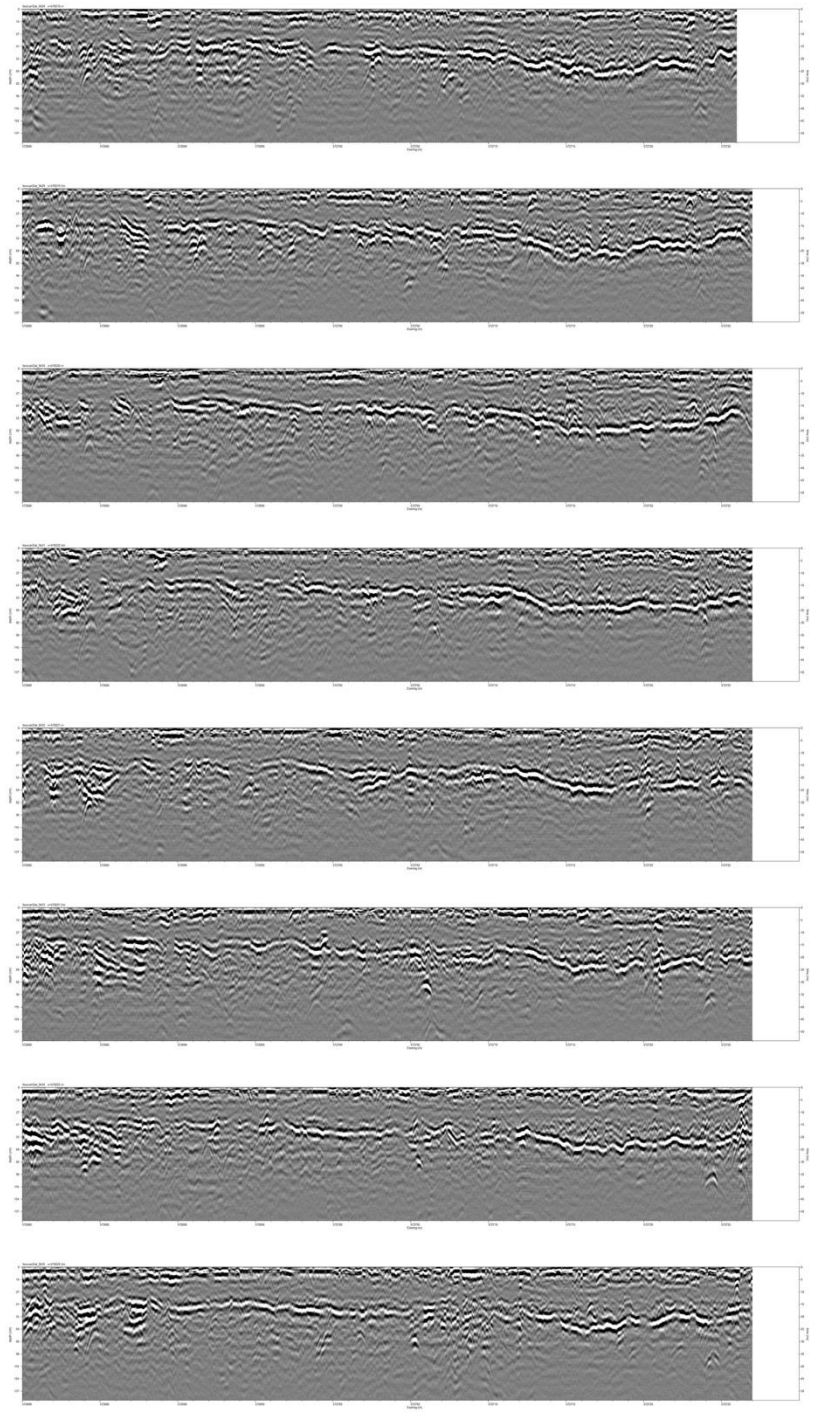

Figure D5. Annotated radargrams for profiles 4928 (478219 E) through 4935 (478222.5E).

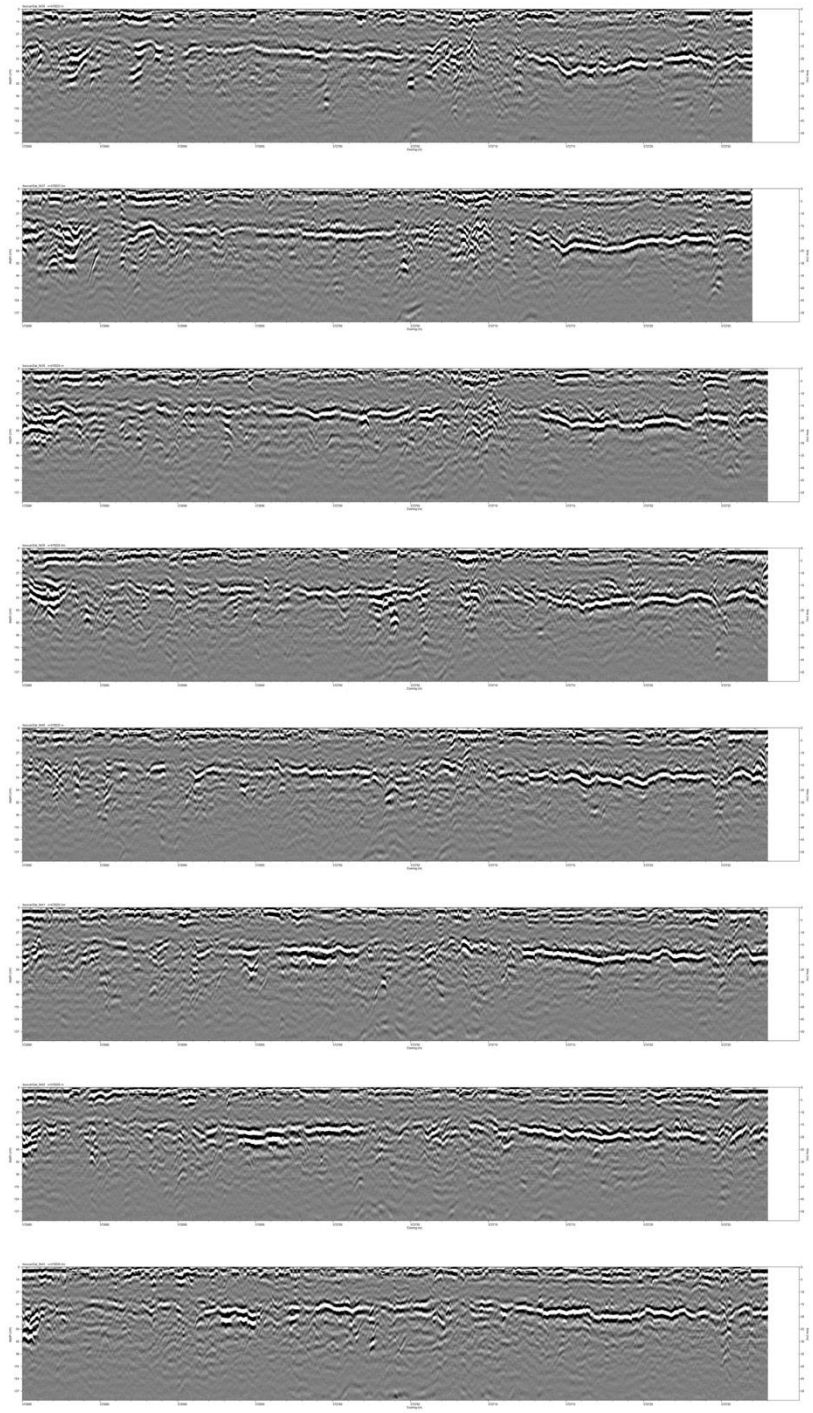

Figure D6. Annotated radargrams for profiles 4936 (478223 E) through 4943 (478226.5E).

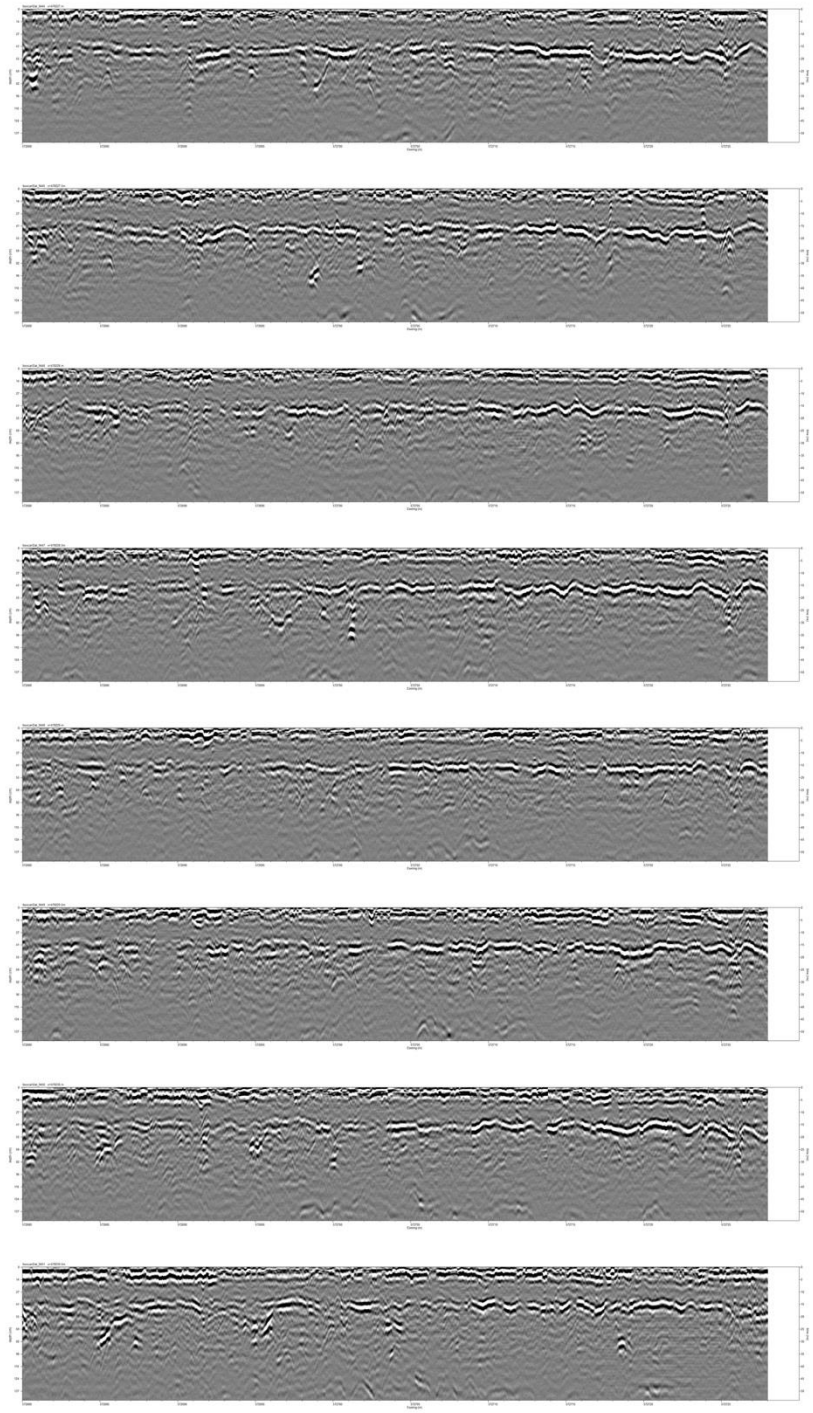

Figure D7. Annotated radargrams for profiles 4944 (478227 E) through 4951 (478230.5E).

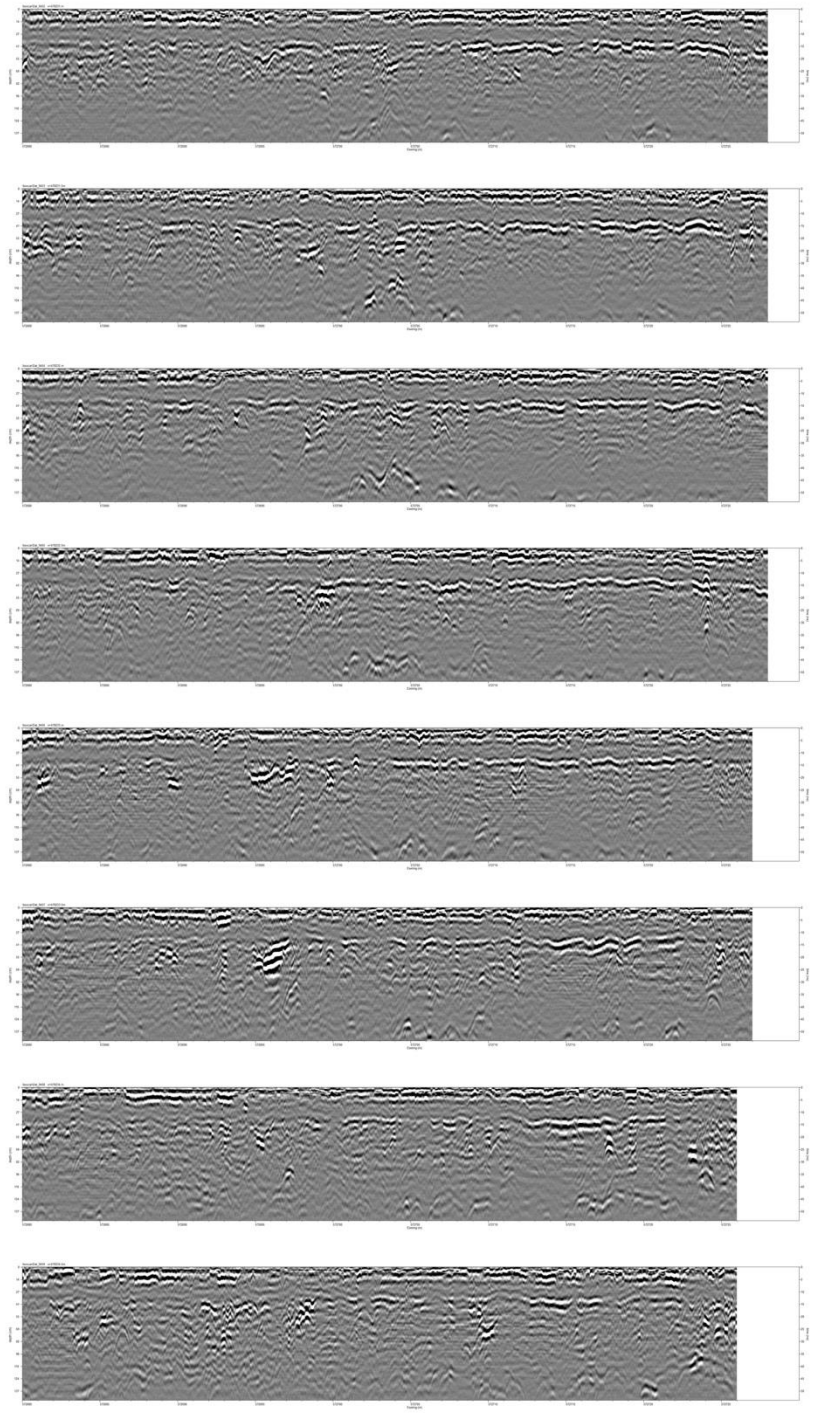

Figure D8. Annotated radargrams for profiles 4952 (478231 E) through 4959 (478234.5E).

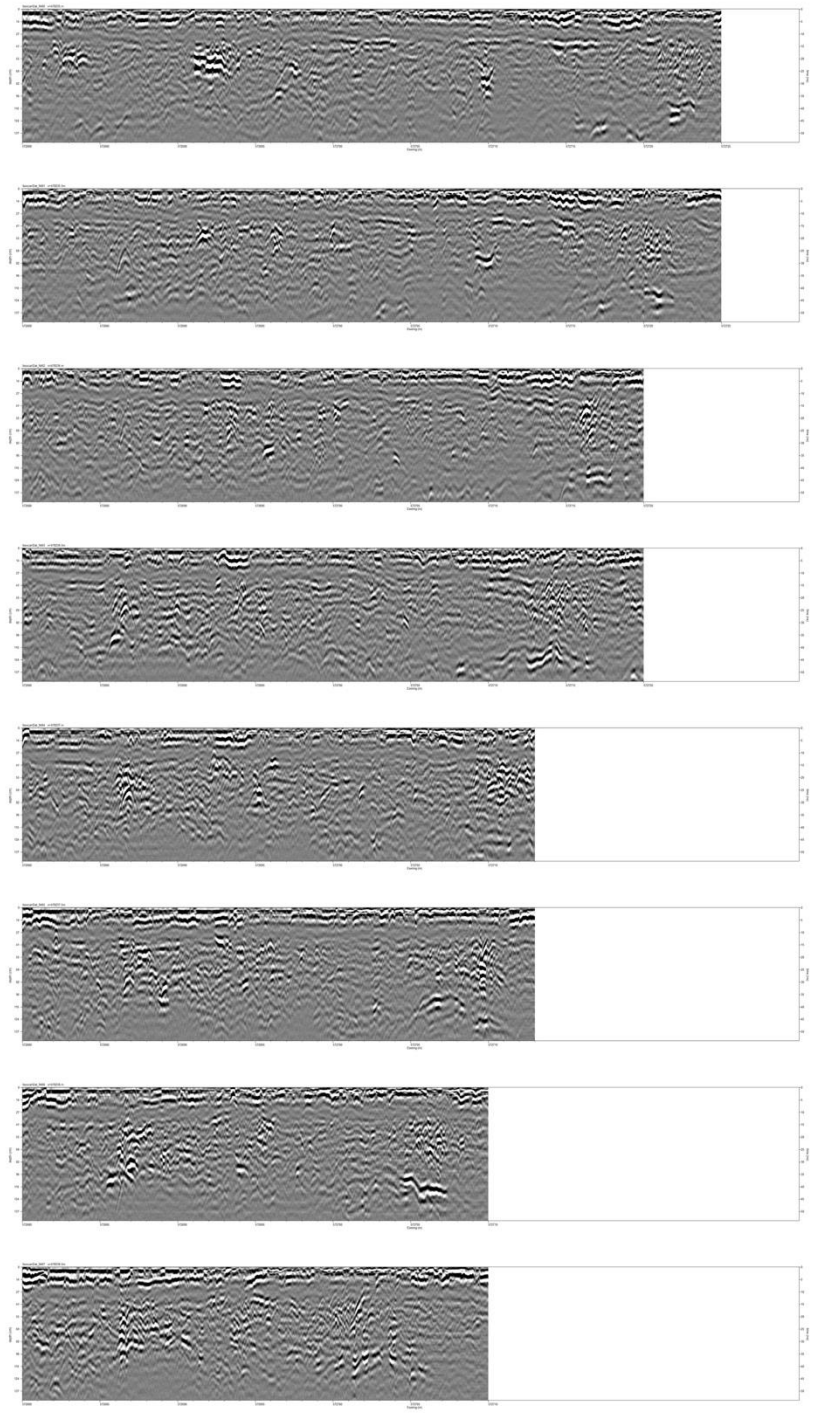

Figure D9. Annotated radargrams for profiles 4960 (478235 E) through 4967 (478238.5E).

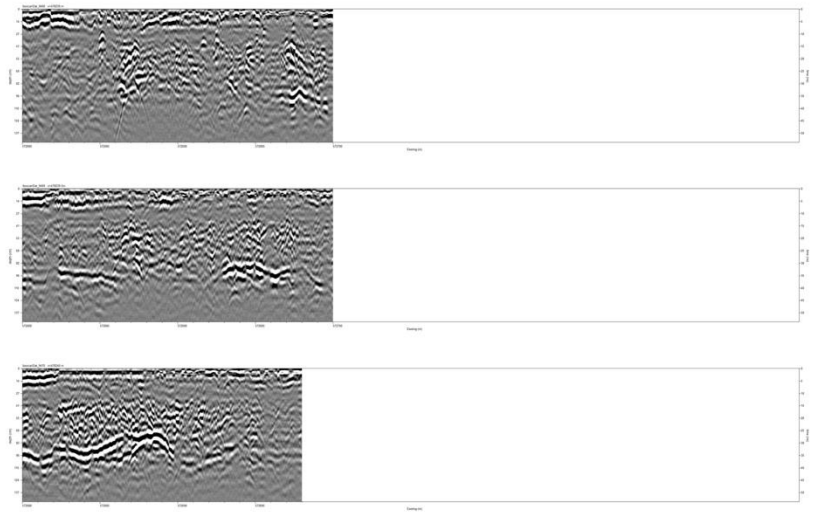

Figure D10. Annotated radargrams for profiles 4968 (478239 E) through 4970 (478240E).

APPENDIX E – GPR SLICES

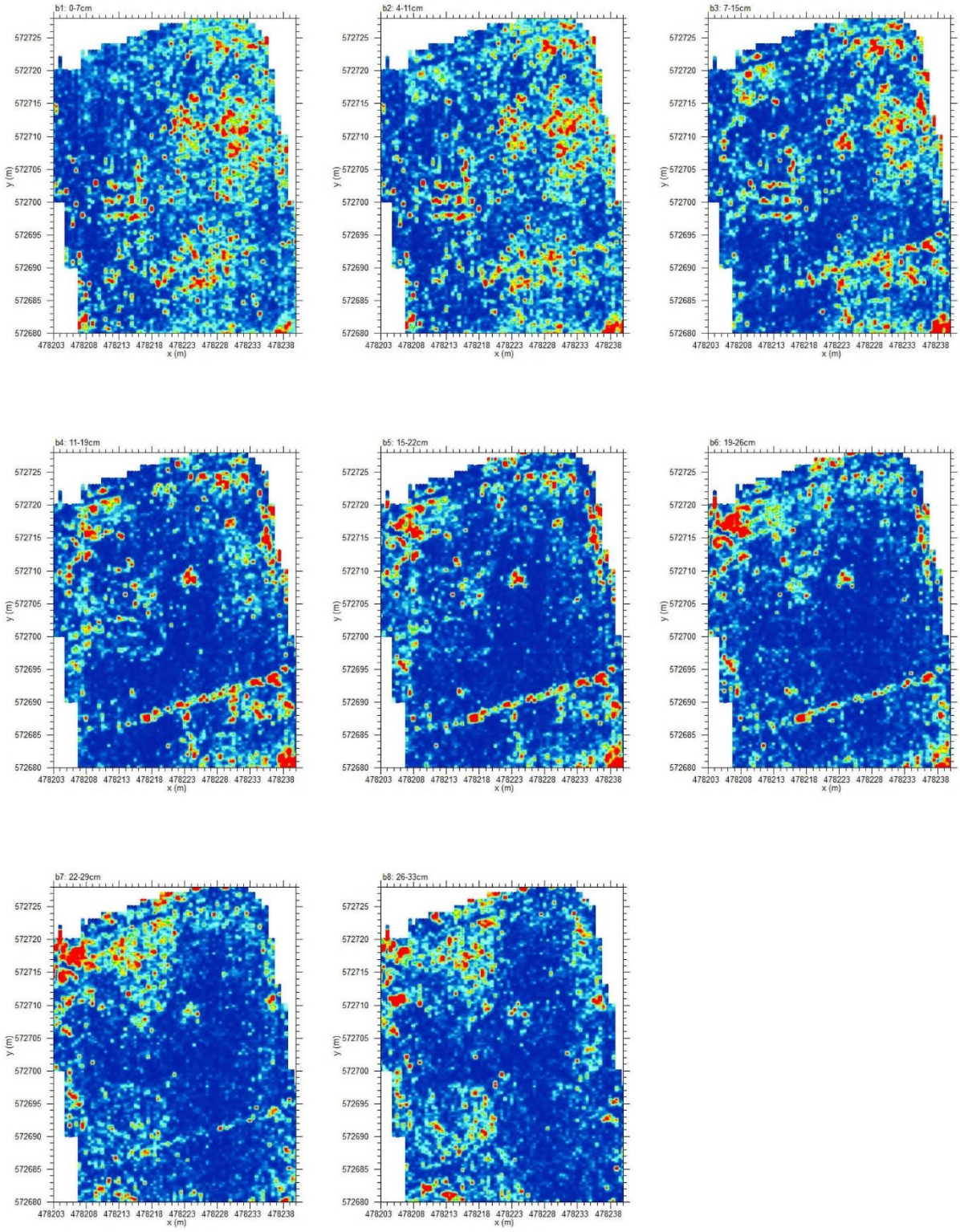

Figure E1. GPR slices 1-8

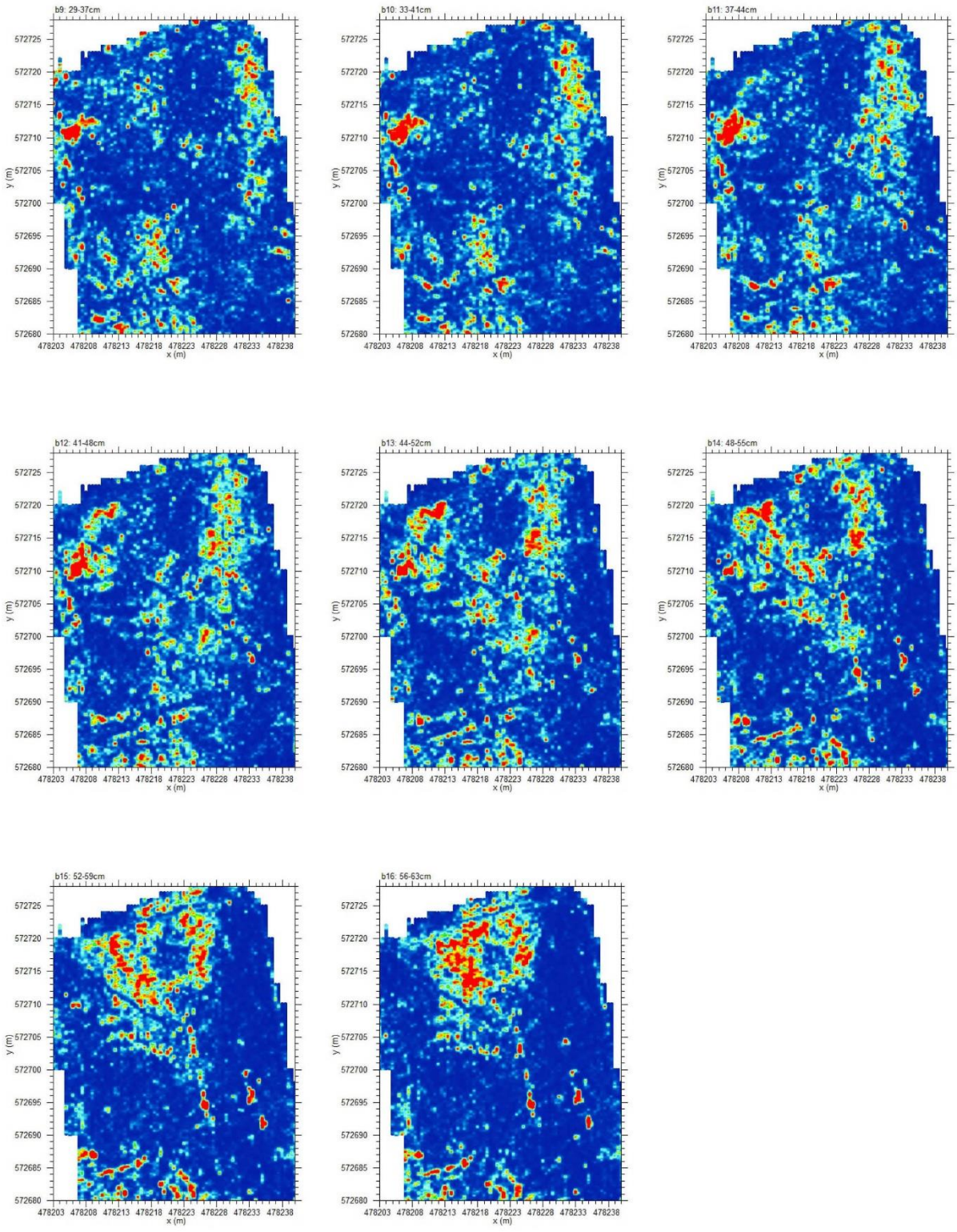

Figure E2. GPR slices 9-16

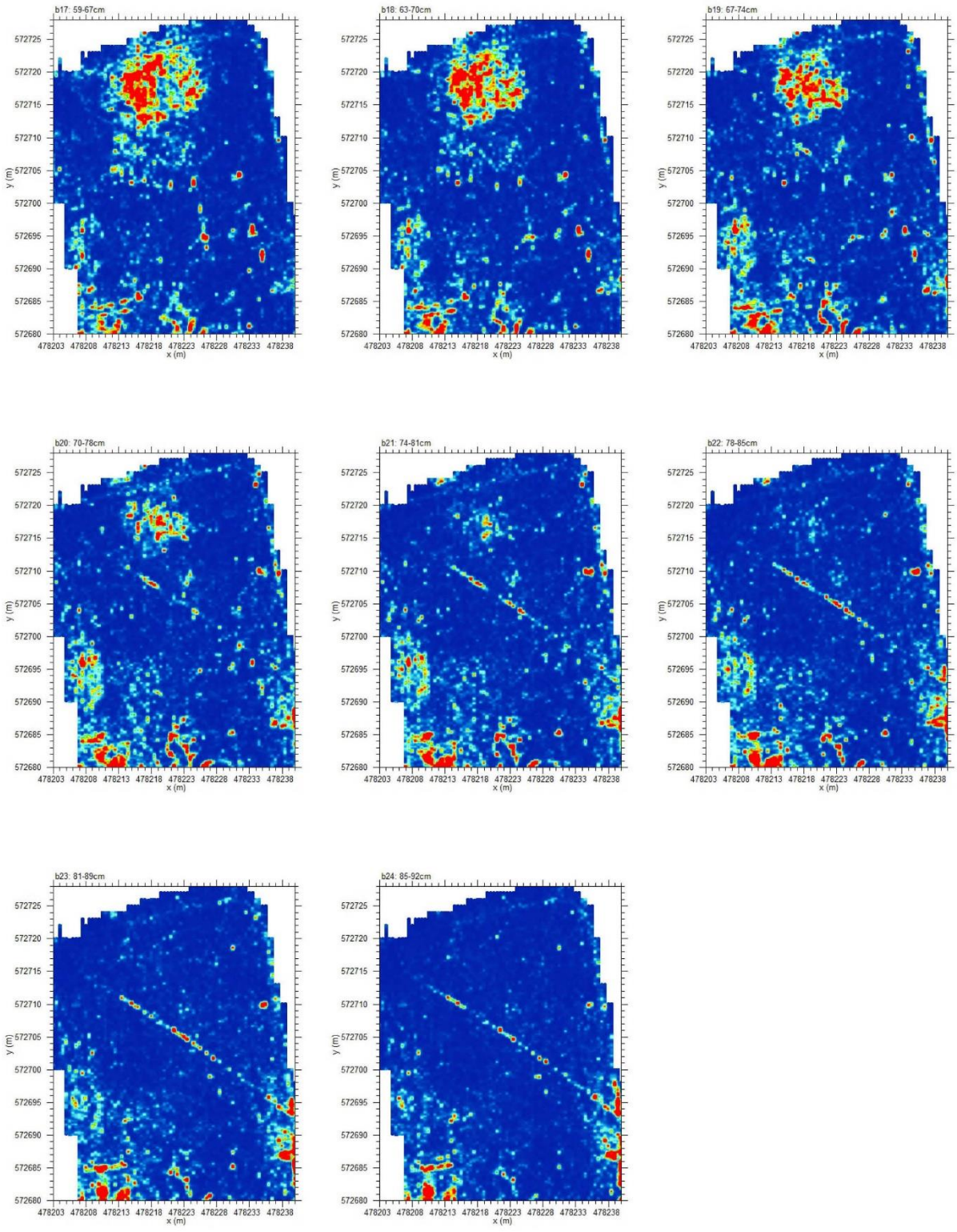

Figure E3. GPR slices 17-24

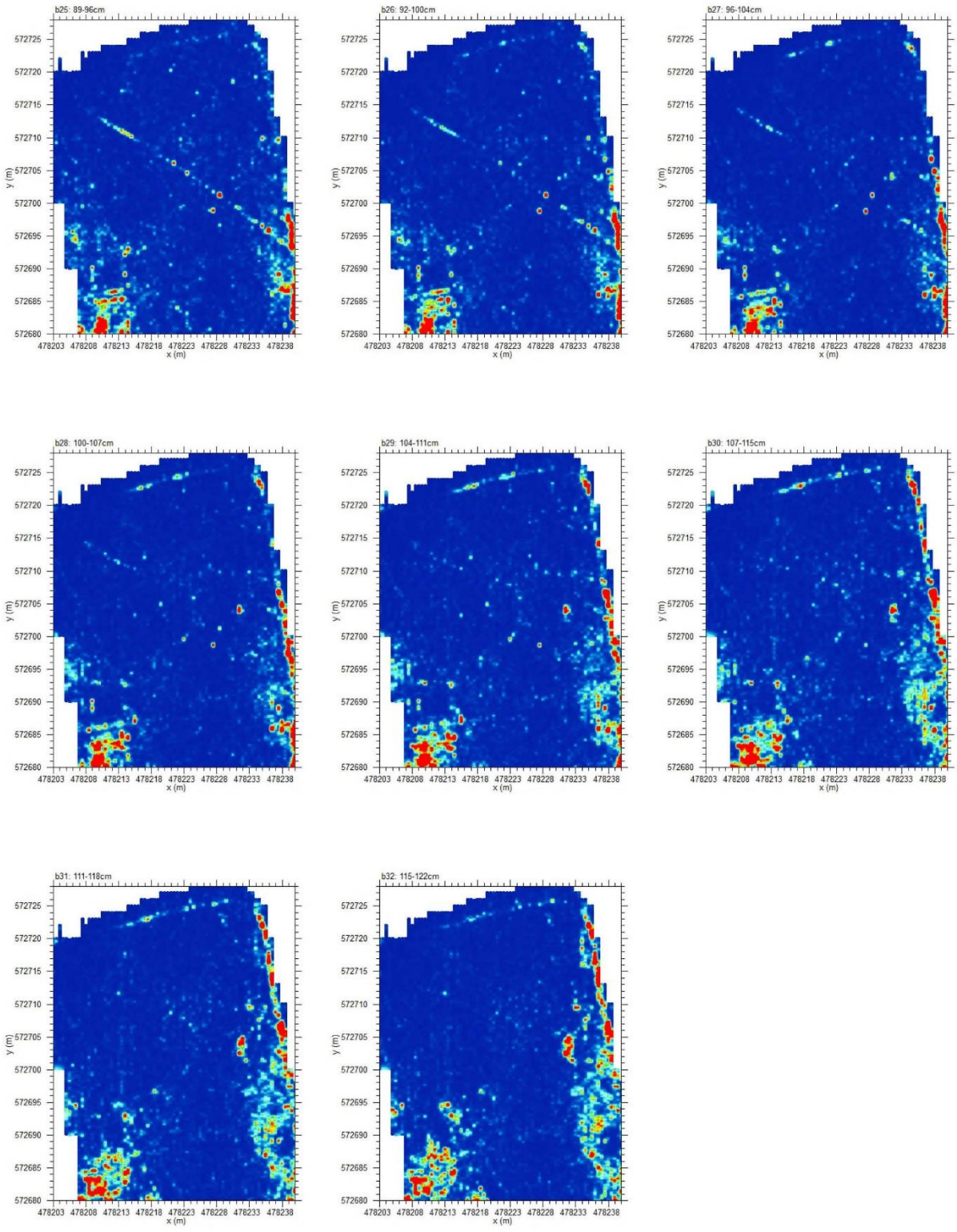

Figure E4. GPR slices 25-32

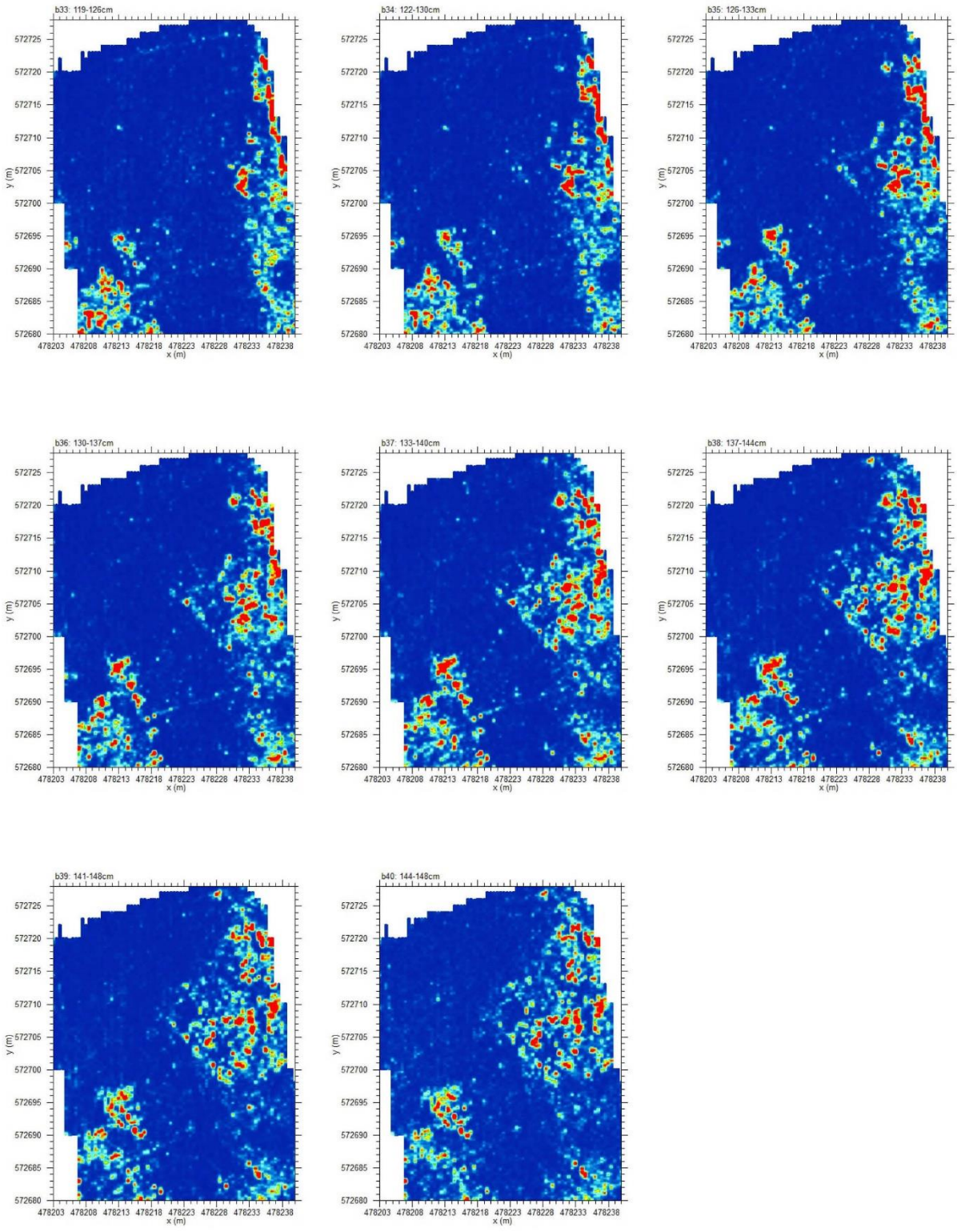

Figure E5. GPR slices 33-40